



TECHNICAL NOTE

# Calculating indicators from global geospatial data sets for benchmarking and tracking change in the urban environment

Eric Mackres, Saif Shabou, and Theodore Wong

## CONTENTS

Abstract .....	1
Introduction.....	2
General methods.....	3
Indicator methods.....	5
General limitations .....	26
Further work .....	27
Endnotes.....	28
References.....	29
Acknowledgments .....	35
About the authors.....	35

*Technical notes document the research or analytical methodology underpinning a publication, interactive application, or tool.*

**Suggested Citation:** Mackres, E., S. Shabou, and T. Wong. 2023. "Calculating indicators from global geospatial data sets for benchmarking and tracking change in the urban environment." Technical Note. Washington, DC: World Resources Institute. Available online at: [doi.org/10.46830/writn.22.00123](https://doi.org/10.46830/writn.22.00123).

## ABSTRACT

Global data sets derived from remote sensing, urban sensors, crowdsourcing, or surveys can provide valuable insights on the current state of cities, how cities are changing, and opportunities to improve the urban environment. This technical note discusses methods for using these data in combination with locally meaningful jurisdictional boundaries to calculate local measurements of indicators on several themes—including access to urban amenities, air quality, biodiversity, flooding, climate change mitigation, heat, and land protection and restoration—relevant to urban decision-makers, researchers, and other stakeholders. These indicators were identified and prioritized in consultation with program staff and stakeholders from two global sustainable urban development initiatives: Cities4Forests and UrbanShift. Indicator calculations were also generated for cities of interest to these initiatives. These indicators can help urban policymakers and civil society assess differences within their cities; make comparisons with other cities; and measure themselves against national or global benchmarks, such as the Sustainable Development Goals, or against self-defined metrics. Geospatial analysis and zonal statistics methods are applied to existing published geospatial data sets and relevant administrative, statistical, or physical city boundaries to calculate comparable indicators for any city or urban area. This methodology can be applied to any area of interest on Earth. Most indicators are based on open-source data, increasing the feasibility of repeating, replicating, and scaling the analyses at low marginal cost. Although the transferability and comparability of these methods are notable strengths of this approach, this note also discusses limitations of this approach for decision-making.

---

## INTRODUCTION

Global data sets derived from sources such as remote sensing, urban sensors, crowdsourcing, or surveys can provide valuable insights on the current state of cities, how cities are changing, differences among cities and among neighborhoods within cities, and opportunities for improvements to the urban environment (Prakash et al. 2020; Helmrich et al. 2021). However, these data are often inaccessible or not immediately relevant to urban stakeholders and decision-makers (Kalluri et al. 2003; Zerger and Smith 2003; Engel-Cox et al. 2004; Wellmann et al. 2020). Processing these data to produce indicators that provide local measurements of themes of interest to local stakeholders is a necessary, yet oftentimes missing, step to enable the supply of new data to meet the demand for locally relevant insights and responsive decision-making (Prakash et al. 2020; Wellmann et al. 2020). Additionally, these indicators can help urban policy-makers and civil society assess differences within their cities; make comparisons with other cities; and measure themselves against national or global benchmarks, such as the Sustainable Development Goals (SDGs), or against self-defined metrics (Kuffer et al. 2018; Avtar et al. 2019; Kavvada et al. 2020; Wang et al. 2020; Giuliani et al. 2021; Song and Wu 2021).

The past few years have seen the beginning of a revolution in remote sensing, crowdsourced data, cloud computing, and machine learning—technologies that are quickly generating new insights about Earth and its urban areas (Fritz et al. 2019; Kavvada et al. 2020; Niu and Silva 2020; Salcedo-Sanz et al. 2020; Ludwig et al. 2021). For the first time, researchers and citizen-scientists have access to globally standardized, open-source, continually updated data sets and methods to help answer important questions about how we live and the impacts of our present and future activities, from the neighborhood scale to the continent scale. This also means that some information that had not been previously collected or made public through local methods (e.g., ground-based tree inventories) can be generated through alternative means, which are often cheaper and easier to implement over large areas (e.g., remote sensing-based tree cover mapping). Moreover, utilizing open-source data increases the feasibility of repeating, replicating, and scaling the analyses for additional cities or time frames at low marginal cost, which can be particularly helpful in data-scarce regions or on topics with limited local data available.

To help understand the status of development and sustainability in cities and identify existing and potential challenges, this paper presents a consistent, replicable approach to calculate indicators on seven key themes: access to urban services and amenities (ACC), air quality (AQ), biodiversity (BIO), flooding

(FLD), climate change mitigation (GHG), heat (HEA), and land protection and restoration (LND). Data to measure these indicators, as described in this document, are almost exclusively taken from global, open-source data sets. However, these methods can be customized by including equivalent local data sets.

Indicators are calculated to assess the baselines and trends of change within each city on identified themes, providing information to distinguish patterns within and between cities and helping to detect problems and define solutions (e.g., prioritizing neighborhoods with limited tree cover for a tree planting campaign). The methods are open source, so other researchers are also welcome to use the methods and scripts developed to process data and make calculations for other cities or with different input data. The results will be disseminated to local and national governments as well as to civil society stakeholders in the context of initiatives supported by WRI Ross Center for Sustainable Cities.

So far, the indicators developed using this framework align with themes of interest to two city cohorts with which WRI Ross Center has been working. The two immediate pilot applications of the indicator methods described in this technical note are for cities participating in the Cities4Forests and UrbanShift initiatives.

- Cities4Forests<sup>1</sup> supports city decision-makers in over 80 cities in making commitments and taking action to preserve and expand tree cover within, near, and far away from their cities. Urban tree indicators can be used by forestry or other tree-focused staff in municipal governments to inform policies and programs related to forests and natural resource management.
- UrbanShift<sup>2</sup> supports city decision-makers across 23 cities on four continents to adopt integrated approaches to urban development, shaping zero-carbon, climate-resilient communities where both people and the planet can thrive. The initiative's focus includes biodiversity, climate change, and land degradation, and we have developed indicators on these themes. We anticipate that city planning and other strategic sustainable urban investment-focused staff in municipal governments will use the indicators to inform policies, programs, and projects in UrbanShift cities.

The themes prioritized and indicators calculated for the city cohorts convened by these initiatives were developed in consultation with their staff and stakeholders. An iterative process involving meetings with and surveys of staff working directly

with city stakeholders in 2022 (Cities4Forests account managers and UrbanShift regional coordinators) provided the main information used to identify the most important and relevant themes, define the indicators, and organize the presentation of the calculations for the cities. Indicator calculations and visualizations for these cities will be made publicly accessible through an online dashboard.

We anticipate that these indicators, and others like them calculated using a similar framework, will be relevant to many other city cohorts and urban themes. Many indicators also align with global objectives, such as the urban targets of the SDGs (SDG 11) (United Nations n.d.). We foresee additional uses of the indicators included in the technical note in other geographies and time frames and the development of supplemental indicators on existing and new themes and using new data sources. Additionally, we expect to update the indicator calculation methodologies for these current city cohorts as new data covering additional years become available.

Some cities may have more granular and detailed relevant data for measuring the themes of our indicators. However, even those cities can benefit from measurements that are standardized globally, between cities, and over time; provide enhanced temporal resolution; and are available worldwide. Additionally, these indicators can provide a screening and prioritization tool. Global data will rarely, if ever, be more useful than local data for monitoring local dynamics, but such data sets can help users understand the main challenges faced locally and start conversations about addressing them. Even when the lower local accuracy levels of global data sets impede local usability, they can help generate the conversations needed to identify local concerns and then identify better data.

Other projects on various urban and nonurban topics have developed indicators using zonal statistics derived from global geospatial data sets (Bocher et al. 2018; Jing et al. 2019; Cochran et al. 2020; Kuffer et al. 2020; Sathyakumar et al. 2020; Boeing et al. 2022; Nicoletti et al. 2022). However, this publication presents the first method of this kind developed by WRI to include multiple urban themes and focus on the needs of specific city cohorts and their questions around urban change, opportunities, and risks.

## GENERAL METHODS

To calculate the indicators, we use a general data management workflow that is consistently applied across all indicators. We also use methods to process specific data relevant to individual indicators. All indicators are assigned short name designations and are organized into themes, as shown in Figure 1. The definitions and methodologies for calculating the indicators in the seven themes below are described in detail in the following sections, which are organized and named by theme.

- Access to urban services and amenities (ACC)
- Air quality (AQ)
- Biodiversity (BIO)
- Flooding (FLD)
- Climate change mitigation (GHG)
- Heat (HEA)
- Land protection and restoration (LND)

These themes and indicators are not intended to be exhaustive; rather, they are tailored to the needs of the specific initiatives for which they were originally developed. We anticipate adding additional indicators under these themes and potentially adding additional themes as identified as important by cities or other stakeholders. All indicators are subject to limitations and uncertainty associated with their methods, as described specifically in each indicator section and generally in the “General limitations” section.

### General data management workflow

Our general data workflow consists of three steps to process, standardize, calculate, and save data, as visualized in Figure 2.

- **Step 1: Define boundaries.** As our indicators consist of zonal statistics, which are statistical descriptive summaries of raster (or grid) data within vector (or polygon) boundaries, we must first define zones. We define zones based on locally relevant administrative boundaries. For each city, we define boundaries for two administrative levels: the overall area of interest (typically a municipality or a metropolitan area) and several subareas (typically multiple wards/districts within a municipality or multiple municipalities within a metropolitan area). The former represents the union into a single polygon of the multiple geographies of the latter. The source of these boundaries may be a polygon file or map received from the local government or obtained from a national statistical agency. If such a local data source is not easily accessed,

Figure 1 | Themes and indicators described in this document

THEMES	Access to urban services & amenities	Air quality	Biodiversity	Flooding	Climate change mitigation	Heat	Land protection and restoration
INDICATORS	Recreational space per capita	Change in air pollutant emissions	Natural areas	Exposure to coastal and river flooding	Greenhouse gas emissions	Extreme heat hazard	Permeable areas
	Urban open space for public use	High pollution days	Connectivity of natural lands	Extreme precipitation hazard	Climate change impact of trees	Land surface temperature	Tree cover
	Proximity to public open space	Fine particulate matter exposure	Biodiversity in built-up areas (birds)	Land near natural drainage		Surface reflectivity	Change in vegetation and water cover
	Proximity to tree cover		Change in number of vascular plant species	Impervious surfaces		Built land without tree cover	Habitat areas restored
			Change in number of bird species	Vegetation cover in built areas			Habitat types restored
			Change in number of arthropod species	Vegetation cover in riparian zones			Protected areas
				Vulnerability of steep slopes			Protection of Key Biodiversity Areas
							Built-up Key Biodiversity Areas

Source: WRI authors.

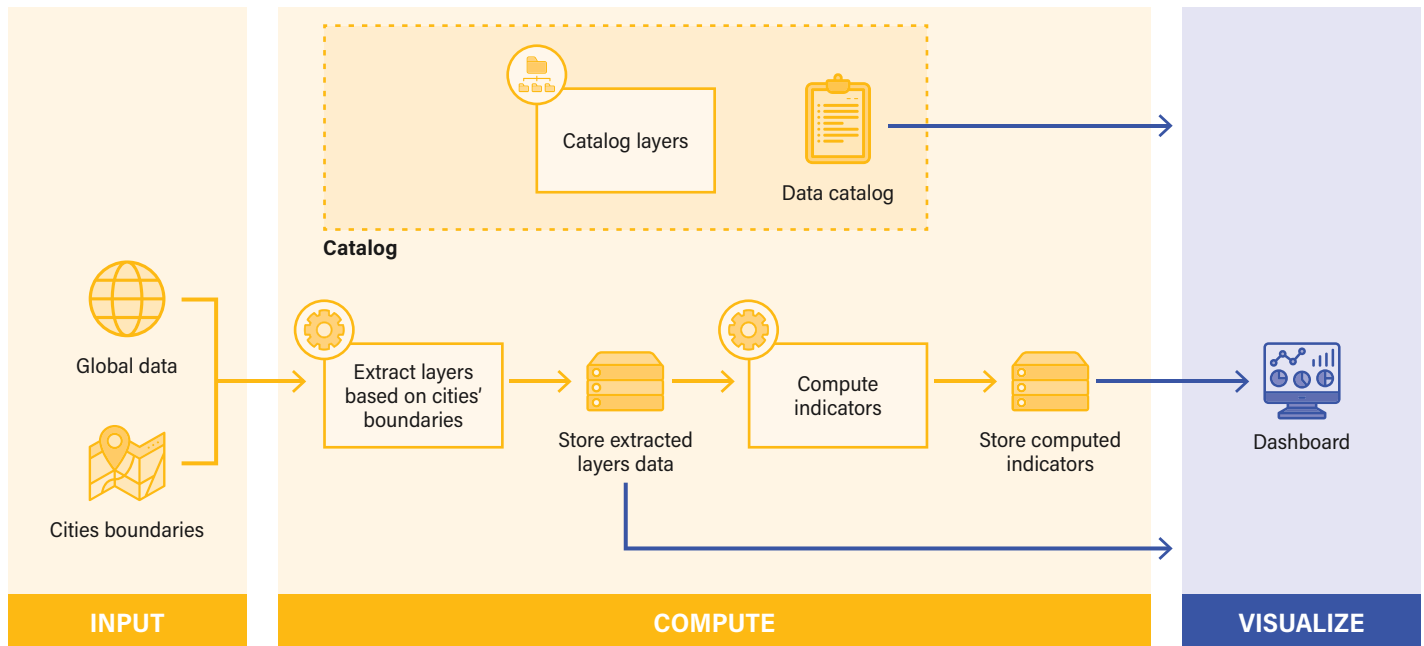
the boundaries may be obtained from a global database such as geoBoundaries (Runfola et al. 2020) or OpenStreetMap (OSM).<sup>3</sup> Where multiple options are available, stakeholders are consulted when possible on the most appropriate boundaries to use. Even for indicators that use a time series of data and for regions where boundaries may have changed over time, we use only the most recent available boundaries for our calculations to hold the region of study constant. These boundaries for each area of interest are then saved as GeoJSON files with a standard naming schema.

- **Step 2: Extract citywide data layers.** The defined boundary extents are used to extract the data for each city area of interest from global data sets relevant to calculating one or more indicator. These extracted data are saved with respect to defined schemas and are stored as GeoTIFF or GeoJSON files depending on the data type: raster or vector, respectively.

Metadata for each data source and extracted subset are also stored as a JSON file.

- **Step 3: Calculate the final indicators.** For each zone defined in Step 1, we run spatial statistic calculations on the data layers, as extracted in Step 2, in keeping with the methods for each specific indicator. For all indicators, we use weighted reduction calculations (using only the portions of pixels that fall within the area of interest) to calculate these zonal statistics, primarily using reduction functions from Google Earth Engine (GEE 2021). We then store the indicator value for each geographic zone in a table aggregated by indicator with respect to a common schema. Next, we produce a final aggregated table with all indicators for all zones relevant to a city cohort. This table can then be used for further statistical analysis, joined with a polygon file of boundaries to produce a map, or integrated into visualization software.

Figure 2 | **General data management workflow**



Notes: The figure describes the steps applied to generate calculations for each city, data source, and indicator. Boundaries are used to extract a spatial subset layer from the source data set that is relevant to the city. This subset is stored, and its metadata is added to a data catalog. The indicator methods are applied to the spatial subset, and the calculation result for each boundary is appended to a table that stores the unique indicator results for each boundary.

Source: WRI authors.

Scripts to implement these methods are saved in code repositories on GitHub.<sup>4</sup>

## Selection of relevant input data sets

For several indicators, multiple potential source data sets could be used. To select the data sets for use in our indicators, we followed a few general principles. We typically chose the data set that met the greatest number of our criteria. In cases where there were trade-offs between multiple criteria, we prioritized the criteria that were most important to enable consistent and meaningful calculations of the specific indicator. The following criteria were used to evaluate data sets:

- Published in a peer-reviewed source
- Open-source license
- Globally consistent coverage
- Recency of data
- High spatial resolution

- High accuracy compared to peer data
- Broad temporal coverage (multiple years of data to enable time series comparisons)
- Likelihood of ongoing support for the source data initiative and future updates to the data set, enabling updates to the indicators and tracking over time
- Compatible spatial and temporal resolution with other data sets used for the indicator

## INDICATOR METHODS

### Access to urban services and amenities (ACC)

Cities exist because the physical proximity of many kinds of activities enables residents to more easily access opportunities and collaborate economically. But access to opportunities varies considerably within cities. These indicators measure the variation in physical access to services and amenities within cities.

---

## ACC-1: Recreational space per capita

### DEFINITION

The hectares of recreational space (open space for public use) per 1,000 people.

### IMPORTANCE

Parks, natural areas, and other open spaces provide city residents with important recreational, spiritual, cultural, and educational services. The use of open and green spaces has been shown to improve human physical and psychological health (Pietilä et al. 2015; Litwiller et al. 2016).

### METHODS

The recreational services indicator is calculated as

$$\frac{\text{total area of recreational space within the boundary}}{\text{population within the boundary} \div 1,000}$$

Data on recreational areas were taken from the crowdsourced data initiative OSM using the Geemap Python library (Geemap n.d.). The OSM tags used to retrieve polygons of these areas are *park*, *nature\_reserve*, *common*, *playground*, *pitch*, and *track* in the leisure category and *protected\_area* and *national\_park* in the boundary category. Population data are 2020 estimates from WorldPop accessed through Google Earth Engine (WorldPop n.d.).

### LIMITATIONS

There is uncertainty in the population estimates, especially the distribution of population within enumeration areas. Analysis of these WorldPop data for Namibia have found large cell-level errors, particularly in areas of informal settlements (Thomson et al. 2022).

## ACC-2: Urban open space for public use

### DEFINITION

The percentage of built-up area that is open space for public use.

### IMPORTANCE

The availability and area of public open space, such as parks, are key factors for assessing the quality of life for city residents. Open spaces provide ecosystem services, recreation opportunities, and habitat for wildlife. Indicators of open space are included in the SDGs (Indicator 11.7.1 [UN-Habitat 2020]) and the Singapore Index on Cities' Biodiversity (Chan et al. 2021).

### METHODS

This indicator uses polygon data on categories of open space as retrieved from OSM in August 2022 using the Geemap Python library (Geemap n.d.). The OSM tags used to retrieve these areas are *park*, *nature\_reserve*, *common*, *playground*, *pitch*, and *track* in the leisure category and *protected\_area* and *national\_park* in the boundary category. For this indicator, we focus on open space that is within urbanized areas of the city and therefore more easily accessible by a greater population. This is distinct from ACC-1, which considers all public open space within the jurisdictional boundary, including in nonurbanized areas. To constrain our analysis to urbanized or built areas of the city (areas where land is predominantly covered by urban infrastructure, such as buildings and streets, and where most people live and work), we use data on these areas as derived from the 2020 European Space Agency (ESA) WorldCover data set's "built-up" class<sup>5</sup> (ESA 2020a; Zanaga et al. 2021). Status as open space or non-open space for each 10-meter (m) pixel of built land is derived using the built-up class as a mask to constrain the analysis to only urbanized areas. Finally, the count of masked pixels of open space divided by the count of all masked pixels is used to calculate the percentage of built area that is open space.

### LIMITATIONS

Because of the relatively high (10 m) resolution of the WorldCover data set and its definition of built-up areas, large- and medium-sized urban open spaces that are predominantly green areas will be excluded. As a result, this indicator best captures smaller open spaces, such as pocket parks; open spaces that are not predominantly green, such as plazas; and designated parks that are a mix of built-up and nonbuilt land, such as historic districts. This indicator is a candidate for future revision to use an alternative urbanized area mask based on a data set that provides a common, global definition of urbanized areas of cities that is less restrictive of green open spaces. From our assessment, a global data set meeting this description is not yet available.

OSM is a crowdsourced data set with a diverse user community, and its completeness, accuracy, and standards of use vary considerably. Accuracy within individual studied cities is not precisely known. Some regions lack data on some of their open spaces in OSM, but all cities we have analyzed so far have data on the sites of at least some open spaces. Additionally, use of the OSM taxonomic system of tags to categorize features is used differently by different local contributing communities. In selecting the tags used in our methods, we considered the most commonly used tags to designate open spaces available for pub-

lic use (parks, athletic fields, etc.) but attempted to exclude tags used primarily for private, limited access or indeterminate open spaces. However, as the OSM tagging system is not designed to make this distinction, this may result in the exclusion of data on some open spaces that are available for public use as well as inclusion of some nonpublic open spaces for some cities. OSM is being constantly edited, potentially improving the relevant data for these cities, so our download of data from one point in time may become outdated. Finally, metadata for OSM features (parks, roads, etc.) include when the feature was added or edited in the map but typically do not provide information on when it was installed on the ground. This makes it difficult to measure changes to cities over time using OSM data.

### ACC-3: Proximity to public open space

#### DEFINITION

The percentage of the population within walking distance (400 m) of public open space.

#### IMPORTANCE

Beyond simply being present, open space must also be easy to access. Although accessibility has many elements, physical proximity to open spaces is an important factor affecting who does or does not have access. The spatial distribution of open spaces across a city, their alignment with population locations, and their accessibility within walking distance (commonly defined at 400 m, including in the Singapore Index [Chan et al. 2021]) are all critical factors for understanding how many city residents are well served by open space.

#### METHODS

This indicator makes use of gridded population at 100 m resolution from the WorldPop project as accessed on Google Earth Engine (University of Southampton n.d.). The open space polygons retrieved from OSM are buffered by 400 m to derive recreation catchment areas. The population within those recreation catchment areas is calculated and then converted to a percentage by dividing that value by the total population of the area of interest.

#### LIMITATIONS

The limitations of OSM data previously described are also relevant to this indicator. Additionally, our approach for calculating access to open space relies on Euclidean distance for simplicity. However, this straight-line measurement is not an accurate characterization of how people travel within cities; it does not account for the orientation of streets or barriers to pedestrian

travel. Because of this reality on the ground, in most cases real pedestrian travel of 400 m will enable access to a smaller area than our methods present.

### ACC-4: Proximity to tree cover

#### DEFINITION

The percentage of the population with an average tree cover of greater than 10 percent within walking distance (400 m) of their homes.

#### IMPORTANCE

Proximity to tree cover is an important indicator of quality green space, whether the trees are in public or private space. Privately maintained trees also provide a variety of public benefits, including improved air quality, heat mitigation, and shade. In addition to providing a range of ecosystem services, urban forests are increasingly recognized for their socioeconomic benefits (Kondo et al. 2017; Martinuzzi et al. 2018, 2021; Volin et al. 2020). This indicator considers all trees within walking distance (400 m) for each resident of the city as a measure of the quality of green space that they interact with during an average day. It also distinguishes between populations with and without walkable access to an average tree cover greater than 10 percent, which is the threshold used by the Food and Agriculture Organization of the United Nations and in SDG 15.1.1 as part of the definition of *forest* (UN-Habitat 2022).

#### METHODS

This indicator uses 10 m resolution tree cover data for the year 2020 from the Trees in Mosaic Landscapes data set<sup>6</sup> (Brandt et al. 2022), which gives tree extent within each 10 m pixel. It also applies the gridded population for 2020 at 100 m resolution from the WorldPop project as retrieved from Google Earth Engine. A neighborhood reduction method using a circular kernel of 400 m radius is applied to the tree cover layer to calculate the mean percentage tree cover within 400 m of each 10 m pixel within the area of interest. This result is then used to mask the population layer to only include 100 m population pixels (or a portion thereof) with an average of greater than 10 percent tree cover within 400 m. The population of this 100 m masked population layer is calculated and then converted to a percentage by dividing that value by the total population of the area of interest.

## LIMITATIONS

The limitations previously described related to the use of Euclidean distance are also relevant to this indicator.

The limitations of Brandt et al. (2022) mean that certain cities may have missing tree cover data due to a lack of cloud-free imagery for 2020 or a lack of valid Sentinel-1 radar imagery, which can happen at the borders of satellite orbits and is common in coastal cities. Cloud removal algorithms used to generate tree cover data sets often have a high quantity of false negatives in cities (pixels that look like buildings but are, in fact, clouds) because clouds and buildings share bright reflectance values. The persistence of cloudy images means that most tree cover data sets underestimate trees in cities because these false negative clouds hide trees in some of the pixels. Brandt et al. (2022) employ a more aggressive approach to cloud removal in cities, resulting in fewer false negatives but less available data. In this data set, trees are defined as woody vegetation with a height of more than 5 m, or woody vegetation with a height of more than 3 m having a defined crown with at least a 5 m diameter. This data set properly excludes nontree crops that may be taller than 3 or 5 m, such as tea, sugar, banana, and cacti, but currently it does not disambiguate plantation trees from nonplantation trees. At present, this data set is only available for 2020 and is limited to countries located within the tropics. In the tropics, the data set was found to have 97 percent user accuracy and 96 percent producer accuracy. Additional limitations and uncertainty related to the tree cover data set is described in the methods paper for *Trees in Mosaic Landscapes* (Brandt et al. 2022).

## Air quality (AQ)

Air quality is a major factor in the physical health of urban residents. Cities both produce air pollution and are impacted by pollution. These indicators measure city contributions to air pollution and resident exposure to pollution.

### AQ-1: Air pollutant emissions and their costs

#### DEFINITION

The percentage change in annual air pollutant emissions from city areas (tonnes) and related social costs (in U.S. dollars), disaggregated by pollutant and sector, between 2000 and 2020.

#### IMPORTANCE

Human activity contributes to air pollution and climate change through greenhouse gas emissions from fuel combustion, industrial processes, and agriculture. This pollution imposes social costs through its negative impacts on human health and

economic productivity. This indicator can help decision-makers and stakeholders identify the most important pollutants emitted locally, the activities responsible for the emissions, and, with multiple years of data, understand emissions trends over time.

## METHODS

This indicator is based on the Global Anthropogenic Emissions data set of the Copernicus Atmosphere Monitoring Service (CAMS) and the Emissions of atmospheric Compounds and Compilation of Ancillary Data (ECCAD) (Granier et al. 2019).<sup>7</sup> The data set provides annual estimates of emissions from 12 sectors of human activity, on a 0.1-degree (approximately 11 kilometers [km]) spatial resolution. The estimates are based on simulations and historical data and are updated intermittently. The included sectors are agriculture (livestock); agriculture (soils); agriculture (waste burning); power generation; fugitive emissions; industry; combustion in residential, commercial, and other settings; ships; solvents; solid waste and wastewater; off-road transportation; and on-road transportation.

We use Google Earth Engine to calculate the emissions from within our areas of interest (city administrative boundaries). We extract annual, sector-disaggregated emissions in tonnes per year for 2000 and 2020 for each of the health-related pollutant species available in the data set: black carbon (BC), methane (CH<sub>4</sub>), carbon monoxide (CO), nitrogen oxides (NO<sub>x</sub>), sulfur dioxide (SO<sub>2</sub>), organic carbon (OC) compounds, ammonia (NH<sub>3</sub>), and non-methane volatile organic compounds (NMVOCs). Because of the coarse resolution of this data set, we only report values for the geographic area of the full city and not for each subcity area.

To combine the emissions of multiple pollutant species to generate a meaningful summary value, we convert tonnes to U.S. dollars based on health-related social costs per tonne (Table 1) as estimated by Shindell (2015) for all pollutant species except NMVOCs. For the social cost of NMVOCs, we used the median value for NMVOCs emitted below an elevation of 100 m in van der Kamp (2017). Van der Kamp's estimates are in 2015€, which we converted to 2015\$ at €1 = US\$1.11. To produce a summary number for the final indicator, we share the percentage change in social costs from 2000 to 2020.

## LIMITATIONS

The emissions data used for this indicator only account for direct emissions from activities within the boundaries of the city (Scope 1 type emissions). This data does not account for emissions associated with electricity used in the city but generated elsewhere (Scope 2) or emissions produced elsewhere associated

Table 1 | **Estimated social cost for major pollutant species**

POLLUTANT SPECIES	SOCIAL COST PER TONNE (US\$)
Black carbon (BC)	62,000 <sup>a</sup>
Methane (CH <sub>4</sub> )	740 <sup>a</sup>
Carbon monoxide (CO)	250 <sup>a</sup>
Carbon dioxide (CO <sub>2</sub> )	0 <sup>a</sup>
Nitrogen oxides (NO <sub>x</sub> )	67,000 <sup>a</sup>
Sulfur dioxide (SO <sub>2</sub> )	33,000 <sup>a</sup>
Organic carbon (OC)	51,000 <sup>a</sup>
Ammonia (NH <sub>3</sub> )	22,000 <sup>a</sup>
Non-methane volatile organic compounds (NMVOCs)	1,172 <sup>b</sup>

Sources: a. Nonclimate health-related costs estimated in Shindell (2015); b. Median cost across four German regions for emissions below 100 meters, as estimated in van der Kamp (2017).

with products or services consumed in the city (Scope 3), such as air pollution from fires in formerly forested areas cleared to produce agricultural commodities consumed in cities, including beef and palm oil. Additionally, this analysis does not provide information on where the social cost of these emissions accrues. Because pollution travels and most costs are associated with pollution exposure, not emissions, many of the costs associated with pollution from the city may be experienced outside the city. The CAMS data set is modeled data based on an ensemble of multiple emissions models and is subject to the limitation of those models. The methods used to develop the CAMS emissions data set are described in Granier et al. (2019).

## AQ-2: High pollution days

### DEFINITION

The annual number of days that air pollutants were above World Health Organization (WHO) air quality standards in 2020.

### IMPORTANCE

Exposure to high concentrations of air pollutants increases the probability of developing serious health conditions, reduced lung function, increased susceptibility to respiratory infections, and aggravated asthma. Long-term exposure increases the probability of developing chronic conditions such as stroke susceptibility, heart disease, and cancer (Kampa and Castanas 2008; Lee et al. 2018). This indicator can help public health officials deter-

mine which air pollutants are present at levels dangerous to human health and how many days each year the population is exposed to them.

### METHODS

The data used for this indicator come from the CAMS Global Reanalysis EAC4 data set (Inness et al. 2019), which combines satellite monitoring of pollutant concentrations with atmospheric modeling to estimate concentrations near the earth's surface.<sup>8</sup> The EAC4 data are provided at approximately 80 km spatial resolution. Because of the coarse resolution of this data set, we only report value for the geographic area of the full city and not for each subcity area.

We report the number of days each city was estimated in 2020 to have a near-surface concentration of air pollutants that exceeds WHO's standards for outdoor air pollutants (WHO 2021). Table 2 outlines the pollutants and standards used.

### LIMITATIONS

The CAMS data has uncertainty related to the limitations of the atmospheric modeling methods used. Additionally, the low resolution of the data set does not allow for analysis of

Table 2 | **WHO standards for outdoor air pollutants**

POLLUTANT SPECIES	AVERAGING TIME (HOURS) <sup>a</sup>	WHO-RECOMMENDED AIR QUALITY GUIDELINE MAXIMUM LEVEL <sup>c</sup>
Nitrogen dioxide (NO <sub>2</sub> )	24	25 µg/m <sup>3</sup>
Sulfur dioxide (SO <sub>2</sub> )	24	40 µg/m <sup>3</sup>
Ozone (O <sub>3</sub> )	8 <sup>b</sup>	100 µg/m <sup>3</sup>
Carbon monoxide (CO)	24	4,000 µg/m <sup>3</sup>
Fine particulate matter (PM <sub>2.5</sub> )	24	15 µg/m <sup>3</sup>
Coarse particulate matter (PM <sub>10</sub> )	24	45 µg/m <sup>3</sup>

Notes: a. The World Health Organization provides additional guidelines for the same pollutants for other averaging times; b. Due to limitations with the Copernicus Atmosphere Monitoring Service data set, for the ozone calculations we used data for the nine-hour window of 6 AM–3 PM. In some parts of the world, the highest level of ozone is reached after 5 PM; c. Pollutant concentrations are given as micrograms per cubic meter (µg/m<sup>3</sup>)

Source: WHO 2021.

subcity geographic units and may introduce uncertainty to the city-scale calculations due to aggregated data from an area larger than the city.

### AQ-3: Fine particulate matter exposure

#### DEFINITION

The annual mean fine particulate matter (PM<sub>2.5</sub>) concentration as a percentage of WHO's air quality guideline for annual exposure.

#### IMPORTANCE

PM<sub>2.5</sub> consists of very small particles that are smaller than 2.5 micrometers (µm) in diameter. (For comparison, a typical human hair has a diameter of 50–70 µm.) PM<sub>2.5</sub> is released from combustion (including fuel combustion in vehicles and power plants, the use of wood and other biomass for cooking and heating, as well as wildfires), degradation of vehicle tires during use, and some chemical processes that occur in the atmosphere. PM<sub>2.5</sub> is a serious health concern because the small size allows PM<sub>2.5</sub> particles to travel deep into human lungs, enter the bloodstream, and cause direct damage to internal organs. Long-term exposure to PM<sub>2.5</sub> leads to increased incidence of heart and lung diseases, cancers, and premature death (Feng et al. 2016; WHO 2021). This indicator can help decision-makers determine how many city residents face long-term exposure to dangerous levels of PM<sub>2.5</sub> and in which neighborhoods these residents live.

#### METHODS

This indicator uses the global surface PM<sub>2.5</sub> V5.GL.02 data set from the Atmospheric Composition Analysis Group at Washington University (van Donkelaar et al. 2021).<sup>9</sup> This data set combines models of atmospheric mixing and chemistry with analysis of imagery from the Moderate Resolution Imaging Spectroradiometer, Multi-angle Imaging SpectroRadiometer, and Sea-viewing Wide Field-of-view Sensor satellite instruments from the National Aeronautics and Space Administration (NASA) to generate estimates of PM<sub>2.5</sub> concentrations near the earth's surface. The data are provided at a spatial resolution of 0.01 degrees, or approximately 1.1 km. Our indicator is based on annual average concentrations for 2020.

We report each district's 2020 average PM<sub>2.5</sub> concentration as a percentage of WHO's air quality guideline (recommended maximum level) for annual exposure: 5 µg per cubic meter (m<sup>3</sup>) (WHO 2021). The annual average is calculated spatially over the area of the district. For example, an average concentration of 15 µg/m<sup>3</sup> would be reported as 300 percent of the WHO standard.

This indicator is based on the WHO annual average concentration recommendation for PM<sub>2.5</sub>, as distinct from the WHO 24-hour average recommendation used in indicator AQ-2.

#### LIMITATIONS

The PM<sub>2.5</sub> data set has uncertainty related to the limitations of the atmospheric modeling methods that it uses. The concentration levels we report cannot be directly translated into health impacts. The health impacts of air pollution are not linearly related to pollutant concentrations, so although higher concentrations are worse for health, concentrations at, for example, 300 percent of the WHO standard should not be interpreted as three times worse than concentrations at 100 percent.

### Biodiversity (BIO)

Cities are often thought of as detrimental to biodiversity—and they can have significant negative impacts related to habitat loss and resource extraction—but cities can also make choices that mitigate biodiversity loss and enhance habitat.

Most of the indicator methods in this category are based on the indicator definitions used in the Singapore Index on Cities' Biodiversity (Chan et al. 2021). The Singapore Index is a widely recognized assessment framework designed to help assess and track biodiversity and its protection within cities. The entire Singapore Index encompasses assessment of biodiversity, access to the societal benefits of biodiversity, and government structures and processes supporting biodiversity. It can be used to assess the status of local biodiversity and the conditions that support it as well as to identify priority areas for future urban biodiversity efforts.

The Singapore Index defines indicators and a scoring method, and cities are invited to adapt the indicators and definitions for their own purposes. It does not provide data for calculating indicator values, and data acquisition and processing can make it difficult for cities to use the Singapore Index. We provide data supporting a subset of the Singapore Index's indicators that address biodiversity and access to benefits. Some of the biodiversity indicators do not measure biodiversity directly but rather conditions that support or harm biodiversity. We have defined and implemented our indicators to adhere as closely as possible to the definitions in the Singapore Index. Our approach prioritizes global, publicly available, and peer-reviewed data sets to develop indicators; however, cities often have access to local data that are of higher quality or are more specifically suited to local contexts and needs.

## BIO-1: Natural Areas

### DEFINITION

The percentage of land that is within natural area land classes.

### IMPORTANCE

Natural areas support biodiversity by providing habitat. They also provide human beings with ecosystem services. The portion of the total city area that is close to a natural state thus provides information about a city's biodiversity and about the benefits provided by biodiversity.

### METHODS

Natural ecosystems, as defined by the Singapore Index, are all areas that are natural and not highly disturbed or completely human-altered landscapes. Examples of natural ecosystems include forests, mangroves, freshwater swamps, natural grasslands, streams, and lakes. Parks, golf courses, cropland, and roadside plantings are not considered natural. This indicator is calculated as the percentage of natural area within the city boundary:

$$\frac{\text{total area of natural, restored, and naturalized areas}}{\text{area of city}} \times 100\%$$

We calculated this indicator using the ESA WorldCover 10 m 2020 V100 land-classification map (Zanaga et al. 2021). We included as natural area all land classified in this data set as trees, shrubland, grassland, herbaceous wetland, mangrove, or moss and lichen.

### LIMITATIONS

- The 2020 WorldCover layer was assessed to have overall accuracy of 74.4 percent (Tsendbazar et al. 2021); this means it includes errors in land cover classification, and these errors are carried through to our characterization of natural and nonnatural lands.
- The WorldCover data set has a spatial resolution of 10 m. For some wildlife species, patches smaller than 10 m might provide useful habitat. WorldCover and our implementation of this indicator could fail to account for these tiny patches.
- Some species have requirements with respect to habitat patch size, plant-community composition, level of vegetation homogeneity, and composition of nearby land. Our method accounts for none of these (or other) potentially important ecological details. Biodiversity planning that

prioritizes particular species or that is informed by a locally implemented ecological assessment should contemplate augmenting our indicators with local ground truthing and habitat classifications defined by local species' requirements.

## BIO-2: Connectivity of natural lands

### DEFINITION

Landscape coherence is a measure of the connectivity of patches of land that can serve as habitat for wild animals. Coherence values range from zero to one, with larger coherence values indicating greater ease of animal movement between habitat patches.

### IMPORTANCE

In general, contiguous habitat benefits biodiversity better than habitat that is subdivided by roads, buildings, and other built infrastructure (Forman and Godron 1991; Fahrig 2003). The connectivity of habitat patches mitigates the effects of habitat fragmentation by allowing wildlife to access more habitat without having to cross inhospitable terrain. The fragmentation of natural areas affects different species differently. For example, a road might not be a barrier for birds, but it can seriously fragment a population of arboreal primates. Although consideration of dispersal ability and habitat requirements are important in the management of particular species, the Singapore Index adopts a generalist approach to quantifying connectivity based purely on patch geometry.

### PLAIN-LANGUAGE CONCEPTUAL DEFINITIONS

**Natural area** is land that is hospitable to wild animals. Because animal species differ in their habitat requirements, the concept of natural area is necessarily nonspecific and is taken by the Singapore Index and by us to encompass natural, near-natural, and other lands that are relatively undisturbed by human activity.

**Connected** natural area patches are patches that are at most 100 m separated from each other at their nearest points. Most animals can move from one habitat patch to another, crossing some distance of inhospitable land. Animal species differ in their movement behaviors and their tolerance of nonhabitat environments, so the Singapore Index uses a generally useful distance to define patch isolation. The 100 m threshold was chosen by a consensus of expert advisers to the development of the corresponding indicator in the Singapore Index.

The indicator is defined as coherence, which is a landscape measure of natural area connectivity. **Coherence** is the probability that any two randomly selected points in a city’s natural areas will be located in the same contiguous natural area patch, or network of connected patches. If the two random points represent the locations of two animals of the same species, the coherence models the probability that they encounter one another. Coherence is the sum of the squared areas of each natural area patch, divided by the squared total natural area. (The areas of patches that are connected to each other are summed and treated as a single patch.) Maximum coherence would indicate a landscape in which all natural area exists as a single contiguous (or connected) patch: coherence would be unity. A landscape in which natural area is subdivided into many isolated patches would have coherence between zero and unity.

## METHODS

We calculated this indicator using the ESA WorldCover 10 m 2020 V100 land-classification map (Zanaga et al. 2021). We included as natural area all land classified as trees, shrubland, grassland, herbaceous wetland, mangrove, or moss and lichen.

The indicator is the coherence

$$Coherence = \frac{1}{A_{total}^2} (A_{G1}^2 + A_{G2}^2 + \dots + A_{Gn}^2)$$

where  $A_{total}$  is the total area of all natural areas;  $A_{G1}$  to  $A_{Gn}$  are the sizes of each group of connected patches of natural area that are distinct from each other; and  $n$  is the total number of groups of connected patches of natural area.  $A_{G1}$  to  $A_{Gn}$  may consist of areas that are the sum of two or more smaller patches that are connected. In general, patches are considered to be connected if they are less than 100 m apart. This equation was derived from Deslauriers et al. (2018).

## LIMITATIONS

- This indicator shares the limitations of BIO-1, which stem from unavoidable errors in land classification.
- This indicator does not currently address roadways as particular dangers to animals, despite the well-documented role vehicle collisions play in harming wildlife (Sugiarto 2022). We would like to integrate roadway information into our implementation of future versions of this indicator.
- We consider two habitat patches to be connected if they are no more than 100 m apart. The 100 m threshold is taken from the definition of the corresponding indicator in the Singapore Index, but its appearance there does not suggest any universal applicability to all types of animal movement.

Some flying animals are likely to tolerate greater distances, and some small animals (especially amphibians) cannot traverse 100 m of, say, pavement. Biodiversity planning that prioritizes particular animals for protection should contemplate implementing this indicator using a distance threshold that accounts for the particular movement behavior and physiological tolerances of the species of interest.

## BIO-3: Biodiversity in built-up areas (birds)

### DEFINITION

The percentage of bird species in all areas that were also observed in built-up areas.

### IMPORTANCE

Cities often include large amounts of built-up and denuded land. These areas are not typically thought of as high-quality habitat, but they can support some species. This indicator reflects the ability of built-up areas to support biodiversity, using birds as an indicator group. Built-up areas include impermeable surfaces such as buildings, roads, and drainage channels as well as anthropogenic green spaces such as roof gardens, roadside plantings, golf courses, private gardens, cemeteries, lawns, and urban parks.

### METHODS

The indicator is calculated as

$$\frac{\text{number of bird species observed in built-up areas}}{\text{number of bird species observed in all areas of city}}$$

To delineate built-up areas, we used the ESA WorldCover 2020 classification of built-up land (Zanaga et al. 2021). For the number of bird species, we estimated the saturation levels of species-area curves as described for indicators BIO-4, BIO-5, and BIO-6, using research-grade observations of birds in 2016–21 in the crowdsourced iNaturalist database, accessed through the Global Biodiversity Information Facility (GBIF 2022b). Calculations are made using only the observations that occurred on built-up land and using all observations within city boundaries. We report the built-up estimate divided by the all-city estimate.

## LIMITATIONS

This method shares the limitations of BIO-4, BIO-5, and BIO-6, as well as the following:

- The WorldCover data set's built-up classification is subject to error due both to automated data processing and to resolution issues.
- All estimates include unavoidable errors. This indicator is calculated from two estimates, and so the potential error is greater. When nearly the entire city or district is built up, the estimated species count on built-up land will be very similar to the citywide estimate, and the indicator value will be close to one. Occasionally, the calculated value is greater than one because of errors introduced by the methods used to produce the numerator, the denominator, or both. In these cases, because values greater than one are impossible, we report the value as one.

## BIO-4–6: Change in number of vascular plant, bird, and arthropod species

### DEFINITION

The estimated change in the number of vascular plant, bird, and arthropod species, 2021–24.

### IMPORTANCE

Direct measurement of biodiversity is important, but it would be impossible to directly assess the diversity and health of all wild populations in a city. We therefore provide species-richness data for the three indicator taxa chosen by the Singapore Index as proxies for overall biodiversity: vascular plants, birds, and arthropods. The change in species richness for these major groups is likely to be directly associated with changes in general habitat quality and in overall biodiversity.

- Vascular plants are plants with vascular tissues, which conduct water, minerals, and the products of photosynthesis throughout the plant. In contrast to nonvascular plants (for example, mosses), vascular plants can grow tall and in locations with little moisture on the surface of the soil. Vascular plants include more than 90 percent of the earth's vegetation.
- Birds are one of the most visible species groups in urban areas, and they are often considered as a key indicator of environmental quality. They are well studied by professional and amateur naturalists worldwide, are sensitive to environmental and habitat changes, and are comparatively easy to observe and count. The Singapore Index includes the change in the number of bird species over time.

- Arthropods include insects, spiders, crustaceans, and other animals with exoskeletons and jointed limbs. They are important actors in terrestrial ecosystems, driving critical processes such as pollination, food-web relations, and nutrient cycling. Many are highly sensitive to changes in their physical and ecological environments.

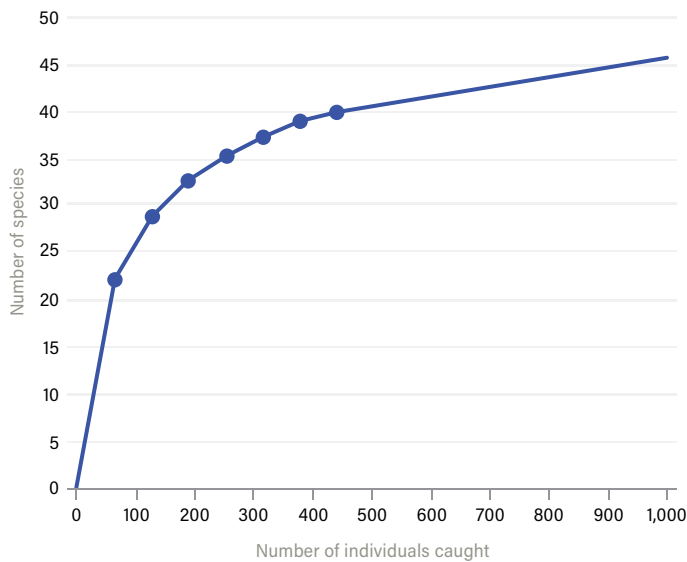
The Singapore Index recommends reporting the number of native species in each of these groups in regular time intervals. A local data collection process would typically involve partnering with a local research institution to carry out a species survey. This survey would be repeated every few years; the indicator is the change in time from a baseline level to the current year. Here, we provide species counts estimated from crowdsourced species-occurrence data sets. Our method cannot substitute for on-the-ground species surveys. We intend it to provide rough estimates that can be used in the absence of more intensive efforts.

### METHOD FOR ESTIMATING SPECIES NUMBER

Biologists often interpret species survey data by examining the number of species found as a function of effort, plotted as a species accumulation curve (SAC). The SAC plots the cumulative number of species recorded as a function of sampling effort (i.e., number of individuals collected or cumulative number of samples). At the start of a species survey, the total number of species found typically grows quickly with every unit of effort. After some time, however, effort expended yields more and more species that have already been found earlier in the survey—and the total number of species grows more slowly per unit of effort. A plot of species number versus effort will come to a plateau, and this saturation level is a common estimator for the number of species in an area, as shown in Figure 3.

We estimated species richness by estimating the saturation level of SACs using individual crowdsourced observations as our effort unit. The estimated counts are the mean saturation levels of 100 SACs, each generated by randomizing the order of all research-grade iNaturalist observations of the Aves (birds), Tracheophyta (vascular plants), and Arthropoda (arthropods) taxa (GBIF 2022a, 2022b, 2022c) in 2016–21. Only species observations with enough data to generate SACs are considered for estimating species richness. Although using just one year of observations might have allowed us to associate species count estimates with particular years, observation data in most cities were insufficient when we limited our method to single-year data. We thus combined data over six years to increase the number of cities for which we could report estimates.

Figure 3 | An example of a species accumulation curve (SAC)



Note: In a field species census, as more individuals are caught, the more unique species are identified. Because the addition of unique species grows more slowly at high capture number, it is possible to extrapolate the curve and estimate a saturation species number.

Source: WRI authors.

## METHOD FOR ESTIMATING CHANGE IN SPECIES NUMBER

The Singapore Index Indicators 4–6 require calculation of changes in species number. At publication time, we have calculated only the baseline species numbers based on iNaturalist data for 2016–21. In a future year, likely 2025, we will estimate species numbers again and report change as an absolute change:

$$change = count_{new} - count_{baseline}$$

We will use the curve-fitting method described above to estimate  $count_{new}$ , but with more recent observation data. For each estimate in 2025, we will use the same number of observations as was used in the corresponding baseline estimate. For example, if the baseline arthropod count estimate for some location was based on 830 observations taken from 2016–21, then we will use 830 observations to estimate the updated arthropod count. We will begin with the iNaturalist observations for the most recent full year, which will be 2024. If the number of observations is less than the number of observations needed, then we will look to 2023. For each year that we do not reach the target observation number, we will look to the previous year. In the year for which the observations become too many if we use the entire set of that year's observations, we will instead use the number of

observations needed, chosen randomly from that year's observations. Because citizen-scientist contributions to iNaturalist have increased over time, we are hopeful that we will be able to match the observation numbers used for the baseline estimate with fewer than six years of observations.

## LIMITATIONS

We use the SAC curve-fitting approach because it is impossible to conduct an exhaustive survey of all species present even in the indicator taxa. However, our reliance on crowdsourced species observations introduces serious limitations.

- Citizen-scientist observations do not benefit from deliberate spatial sampling techniques. One consequence is that the observations that inform our calculations tend to be clustered in heavily populated areas and popular recreational sites. We are therefore likely to miss species that tend to avoid human activity. This probably biases our estimates toward undercounts.
- Our curve-fitting method includes a step that randomizes the sequence in which observations are incorporated into the SAC. Because of the randomization, calculating any of these indicators twice with the same data generally yields slightly different values. We try to minimize the randomization effects by averaging over 100 instances of the curve-fitting step, but we are unable to eliminate the effect entirely.
- In many cities and subcity areas, there are not enough citizen-scientist observations to estimate a plausible SAC. This can be true for any number of the indicator taxa. When there is insufficient data, we are unable to report a species count estimate.
- We are unable to distinguish between native and introduced species. Our estimates almost certainly include introduced species, and in this way our indicators differ from their counterparts in the Singapore Index. Introduced species can (but do not always) harm native populations and ecosystems, and so a large species count—if it does not exclude introduced species—should not be taken as an unambiguous signal of good ecological health.

## Flooding (FLD)

Most cities are sited based on access to water or for use in agriculture, power, transportation, or other purposes. But proximity to water also exposes cities to risks of flooding, which are expected to increase in most of the world with a changing climate. These indicators measure city exposure to a variety of flooding-related risks.

## FLD-1: Exposure to coastal and riverine flooding

### DEFINITION

The percentage of built land exposed to coastal or riverine flooding.

### IMPORTANCE

Most cities are built near coasts or along rivers. These natural assets for economic development can also present a hazard when they cause flooding in built-up areas. The prevalence of these floods is increasing globally due to sea level rise, extreme precipitation, and snowmelt caused by climate change.

### METHODS

We use projections from Aqueduct Floods (Ward et al. 2020), with a resolution of 30 arc seconds (approximately 1 km), retrieved through Google Earth Engine to characterize the coastal and riverine flood hazards for each city in 2050 in terms of meters of expected inundation depth for a given scenario.<sup>10</sup>

The scenario variables we use are a 100-year return period (providing the expected depth of inundation from a once-in-100-years flood event), the business-as-usual/pessimistic (Representative Concentration Pathway 8.5) climate scenario, high sea level rise, no subsidence, and the mean inundation depth from the results of all five riverine projection models that are available in Aqueduct Floods. We then compare locations of either projected coastal or riverine flooding to built-up areas in the city in 2020 as defined by the built-up class from the ESA's WorldCover. For each city and city district, we calculate the number of built-up pixels and the number of built-up pixels projected to experience a flood inundation depth greater than zero under the described flooding scenario. Then we calculate the percentage of built-up pixels with flood exposure.

### LIMITATIONS

The Aqueduct Floods data set with a 1 km resolution may be too coarse for some applications related to assessing flood risk to individual blocks and buildings. Additionally, because this indicator considers 2020 built-up areas in comparison to projected 2050 inundation, it may underestimate built area exposed to the hazard as a result of future land development. Note, however, that this is an indicator of flood hazard, and it does not consider how mitigation measures such as flood protection infrastructure (levees, etc.) may impact the risk of inundation from flooding under the scenario described. This indicator is limited in scope to riverine and coastal flooding hazards, which are modeled independently—combined effects from riverine and coastal floods are not included. It also does not describe hazards from flash pluvial flooding resulting from heavy precipitation events.

## FLD-2: Extreme precipitation hazard

### DEFINITION

The expected extreme precipitation event hazard (expected maximum millimeters of precipitation in one day in 2050) and trend (percentage change between 2020 and 2050 in millimeters of precipitation on the most extreme day).

### IMPORTANCE

Understanding the hazard presented by extreme precipitation and the likely future change of that hazard can inform the importance of planning for extreme precipitation events and investing in infrastructure, such as trees and other vegetation, that can help mitigate their impacts.

### METHODS

This indicator is calculated as

$$\frac{x_{2050} - x_{2020}}{x_{2020}} \times 100$$

where  $x_{year}$  is the expected precipitation on the day of *year* with the most precipitation. The expected maximum daily precipitation is calculated from a probability distribution model using European Centre for Medium-Range Weather Forecasts atmospheric reanalysis (ERA5)<sup>11</sup> historical precipitation data (Hersbach et al. 2020) and NASA Earth Exchange Global Daily Downscaled Climate Projections (NEX-GDDP) ensemble climate projections<sup>12</sup> (Thrasher et al. 2012). In our implementation, the indicator is processed for the 0.25-degree pixel containing the city centroid. Because of the coarse resolution of this data set, we only report value for the geographic area of the full city and not for each subcity area.

More detailed documentation of these methods is under development, and we plan to publish it in a future technical note.

### LIMITATIONS

This indicator is based on estimates of precipitation magnitude probabilities as modeled by climate simulations. There are unavoidable errors from numerous sources, including climate stochasticity, scientific uncertainty regarding Earth system processes, and uncertainty in future greenhouse gas emissions trends. Notably, we use the expected value of a random variable to capture information about a probability distribution in a single number. It should not be interpreted as a prediction.

The two years over which we calculate change might not be appropriate for local planning needs. This indicator only compares expected precipitation for two years; thus, it provides a conservative estimate of risk. The risk is likely higher if multiple adjacent years are considered because the greatest daily precipitation amount between a range of years (e.g., 2046–55) is likely higher than the greatest precipitation expected for just one year (e.g., 2050).

Maximum daily precipitation also is not a direct predictor of flooding. It does not account for aggravating or moderating factors such as antecedent rainfall, the local geography of impervious surfaces or stormwater management systems, and topography.

### FLD-3: Land near natural drainage

#### DEFINITION

The percentage of built land cover within 1 m height above the nearest drainage.

#### IMPORTANCE

Land near natural drainage (e.g., streams, rivers) is at risk for pluvial or flash flooding hazards. Development closer in elevation to natural drainage, especially near drainage for large land areas, is at greater risk. The risk for these types of floods can be difficult to predict, and beyond height above drainage, other factors—such as the amount of precipitation, soil type, extent of impervious surfaces, distance from natural drainage, and the presence and efficacy of built drainage systems—are also important influences.

#### METHODS

This indicator uses 30 m resolution data on height above drainage channels from the Global 30 m Height Above the Nearest Drainage data set<sup>13</sup> (Donchyts et al. 2016) to estimate the land area 1 m or less above the nearest drainage for drains with a flow accumulation area of at least 1 km<sup>2</sup>. We then compare these areas to built-up areas in the city as defined by the built-up class from the ESA WorldCover for 2020.<sup>14</sup> For each city and city district, we calculate at 10 m scale the number of built-up pixels and the number of built-up pixels within 1 m of the nearest drainage. Then we calculate the percentage of built-up pixels that are 1 m or less above the nearest drainage.

#### LIMITATIONS

Although this indicator is an important factor related to flash flooding hazards, it does not include other important information essential to assessing flash flood hazards (soil type, artificial

drainage systems, etc.) comprehensively. The resulting spatial analysis should not be interpreted as a hazard map. Because it does not incorporate data on artificial drainage networks and the city's conveyance and routing of water (sewers, drains, canals), this analysis does not provide a comprehensive picture of where water is going and where it is likely to stagnate during pluvial flooding; rather, it provides only an extremely rough approximation.

### FLD-4: Impervious surfaces

#### DEFINITION

The percentage of built land that has impervious surfaces.

#### IMPORTANCE

Impervious surfaces (in urban areas, typically buildings, roads, and other pavement) prevent water from soaking into the ground on-site and contribute to decreased overall water infiltration and increased runoff and can increase the prevalence of localized flooding. This type of flooding also lowers the quality of receiving waters fed by surface water runoff, impacting the biodiversity of aquatic and marine systems downstream. Building cities in ways that minimize impervious surfaces (with alternative construction materials or intentional greening) allows for greater natural water infiltration and can enable cities to “sponge” up excess water, decrease the risk of flooding, and recharge groundwater resources.

#### METHODS

We obtain the estimated extent of impervious areas in 2018 from the Tsinghua annual maps of global artificial impervious area (Gong et al. 2020).<sup>15</sup> This 30 m resolution data set defines a pixel with at least 50 percent estimated impervious surface as being impervious. We then compare these areas to built-up areas (human settlement areas) in the city as defined by the built-up class from the 2020 ESA WorldCover. For each city and city district, we calculate the number of built-up pixels and the number of impervious built-up pixels at a 10 m scale. Then we calculate the percentage of built-up pixels that are impervious. This indicator is similar to LND-1, with two distinctions. This indicator considers only built-up land in the area of interest (not all land), and the numerator in the calculation is impermeable area (not permeable area).

#### LIMITATIONS

These calculations are based entirely on remotely sensed data, which are not assessed against local ground truth data. The two data sets compared are in different resolutions and assess different years, which presents difficulties for precise comparison.

## FLD-5: Vegetation cover in built areas

### DEFINITION

The percentage of built land cover without vegetation.

### IMPORTANCE

Vegetation cover provides many benefits in urban areas. For flood mitigation, greater vegetation cover can increase water infiltration into the ground, reducing water stagnation and runoff on the surface. In turn, an absence of vegetation cover can increase the prevalence of localized flooding.

### METHODS

To estimate vegetation cover, we used a 10 m annual greenest pixel mosaic of Sentinel-2 imagery (ESA 2015b) for 2020 to calculate the normalized difference vegetation index (NDVI) with a minimum threshold of 0.4, which is commonly used as the threshold for a moderate degree of vegetation (EOS Data Analytics 2019). This NDVI provides an estimate of the location of all types of vegetation within the area of interest. This is distinct from tree cover data (Brandt et al. 2022) used in other indicators, which intentionally includes only trees. We then compare these areas to built-up areas in the city as defined by the built-up class from the 2020 ESA WorldCover. For each city and city district, we calculate at 10 m scale the number of built-up pixels and the number of vegetated built-up pixels. Then we calculate the percentage of built-up pixels that are vegetated.

### LIMITATIONS

These calculations are based fully on remotely sensed data, which are not assessed against local ground truth data. An annual mosaic is used to assess the greenest point in the year for each individual pixel; as a result, this assessment does not measure the state of vegetation at any one point in time but rather the maximum state of vegetation during the year. This estimates for each pixel a combination of the amount of vegetation and state of greenness at peak greenness. In most pixels, the amount of vegetation does not change (except for leaves), but using the peak greenness allows us to estimate how much vegetation exists. Temporal and seasonal changes in vegetation (for example, vegetation that sheds foliage or goes dormant seasonally) are known to affect the ability of green space to deliver expected benefits such as stormwater mitigation. The benefits in areas with seasonal change will not be as high as those in evergreen ecosystems or where there is no seasonal change (Wilson et al. 2022).

## FLD-6: Vegetation cover in riparian zones

### DEFINITION

The percentage of riparian areas without vegetation or water cover.

### IMPORTANCE

Riparian areas—the spatial interface between land and water, particularly rivers and streams—can serve as natural infrastructure for flood control. Whereas in many urban areas these areas have been developed, paved over, or channelized, the presence of vegetation cover in the riparian zone is a primary factor in determining its flood mitigation effectiveness; vegetation can slow down water flow as well as increase its absorption into land and its transpiration into the air (Croke et al. 2017). Riparian areas are also critical habitats that support biodiversity.

### METHODS

This indicator uses data on elevation and drainage channels from the Global 30m Height Above the Nearest Drainage data set and on the location of water bodies from the Joint Research Centre (JRC) Global Surface Water data set<sup>16</sup> (Pekel et al. 2016) to estimate the location of lakes, rivers, and streams. To estimate riparian zones, we buffered these waterways by 144 m—the estimated size of riparian areas often needed to preserve significant bird diversity (Lind et al. 2019)—and excluded the area of the water channel itself. To estimate vegetation and water cover, we used an annual greenest/bluest pixel mosaic of Sentinel-2 imagery to calculate the NDVI and the normalized difference water index (NDWI) with minimum thresholds of 0.4 and 0.3, respectively (McFeeters 2013; EOS Data Analytics 2019). For the buffered riparian areas in each city or subcity unit, we calculated at 30 m scale the count of all riparian area pixels and the count of riparian area pixels with vegetation or water cover. Then we calculated the percentage of riparian area pixels without vegetation or water cover.

### LIMITATIONS

These calculations are entirely based on remotely sensed data, which are not assessed against local ground truth data. In particular, the general definition of *riparian zone* used may not match the situation on the ground as characterized with additional local data, such as in the case of extreme topography adjacent to drainage channels.

---

## FLD-7: Vulnerability of steep slopes

### DEFINITION

The percentage of steep hillside slopes without vegetation cover.

### IMPORTANCE

Steep slopes are vulnerable to landslides, especially during incidence of extreme precipitation or flooding, where soil can become saturated with or washed away by water. Vegetation is critical for stabilizing slopes; roots hold soil in place, and plants absorb water from the soil. Steep slopes without vegetation cover are particularly vulnerable to erosion, which can undermine the entire slope's stability and lead to landslides.

### METHODS

To estimate slopes on land, we apply the Google Earth Engine slope algorithm (GEE 2022) to the global NASA NASADEM 30 m digital elevation model (NASA JPL 2020). The slope layer is then masked to only include high slope areas of 10 degrees or greater—the threshold at which landslide susceptibility starts to grow quickly (Stanley and Kirschbaum 2017). Vegetation cover is estimated using Sentinel-2 imagery<sup>17</sup> to calculate greenest pixel NDVI with a minimum threshold of 0.4—the minimum NDVI value representative of significant vegetation cover (EOS Data Analytics 2019). For the high slope areas in each city or subcity unit, we calculated at 30 m scale the count of all high slope pixels and the count of high slope pixels with any 10 m Sentinel-2 subpixels not meeting the NDVI threshold for vegetation cover. Then we used these values to calculate the percentage of high slope pixels without vegetation cover.

### LIMITATIONS

These calculations are entirely based on remotely sensed data, which are not assessed against local ground truth data. The digital elevation model is based on data collected in 2000, which may be outdated if significant changes have occurred in local slopes. Additionally, its relatively low resolution (30 horizontal m) may not capture important smaller slope details.

## Climate change mitigation (GHG)

Cities are responsible for most human-produced greenhouse gas emissions, but cities are also efficient at using resources and can reduce emissions through innovations to mitigate climate change. These indicators consider how cities contribute to climate change, including by measuring the contribution of economic sectors, gases, and activities.

## GHG-1: Greenhouse gas emissions

### DEFINITION

The change in annual greenhouse gas emissions (CO<sub>2</sub> equivalent [CO<sub>2</sub>e]) from city area, 2000–20 (percentage), disaggregated by pollutant and sector.

### IMPORTANCE

Human activity contributes to air pollution and climate change through greenhouse gas emissions from fuel combustion, industrial processes, and agriculture. This indicator can help decision-makers and stakeholders identify the most important pollutants emitted locally, the activities responsible for the emissions, and, with multiple years of data, emissions trends.

### METHODS

Similar to indicator GRE-2.1, this indicator is based on the CAMS Global Anthropogenic Emissions data set (Granier et al. 2019). The data set provides estimates of emissions from 12 sectors of human activity, on a 0.1-degree (approximately 11 km) spatial resolution. The estimates are based on simulations and historical data. The included sectors are agriculture (livestock); agriculture (soils); agriculture (waste burning); power generation; fugitive emissions; industry; combustion in residential, commercial, and other settings; ships; solvents; solid waste and wastewater; off-road transportation; and on-road transportation.

We used Google Earth Engine to calculate the emissions from within our areas of interest (city administrative boundaries). We extract annual, sector-disaggregated emissions in tonnes/year for 2000 and 2020 for each pollutant species. We also provide summaries of total emissions for 2000 and 2020. Because of the coarse resolution of this data set, we only report value for the geographic area of the full city and not for each subcity area. To have a shared unit of measurement for all species of emissions, we convert tonnes to CO<sub>2</sub>e based on the 20-year global warming potentials (EPA n.d.) as listed in Table 3. To produce a summary number for the final indicator, we share the percentage change in CO<sub>2</sub>e from 2000 to 2020.

### LIMITATIONS

The emissions data used for this indicator only account for direct emissions from activities within the boundaries of the city (Scope 1 type emissions). These data do not account for emissions associated with electricity used in the city but generated elsewhere (Scope 2) or emissions produced elsewhere associated with products or services consumed in the city (Scope 3). The CAMS data set is modeled data based on an ensemble of mul-

Table 3 | Global warming potential of major pollutant species

POLLUTANT SPECIES	INCLUDED AS GHG	GWP (20-YEAR CO <sub>2</sub> EQUIVALENT)	GWP SOURCE
Black carbon (BC)	Yes	460	Global values reported in IPCC AR5, Table 8.A.6
Methane (CH <sub>4</sub> )	Yes	84	IPCC AR5, Table 8.A.1
Carbon monoxide (CO)	Yes	7.65	Midpoints of global values reported in IPCC AR5, Table 8.A.4
Carbon dioxide (CO <sub>2</sub> )	Yes	1	Definition of GWP
Nitrogen oxides (NO <sub>x</sub> )	Yes	19	Global values reported in IPCC AR5, Table 8.A.3
Sulfur dioxide (SO <sub>2</sub> )	No	NA	NA
Organic carbon (OC)	Yes	-240	Global values reported in IPCC AR5, Table 8.A.6
Ammonia (NH <sub>3</sub> )	No	NA	NA
Non-methane volatile organic compounds (NMVOCs)	Yes	14	Global values reported in IPCC AR5, Table 8.A.5

Notes: GHG = greenhouse gas; GWP = global warming potential; IPCC AR5= Fifth Assessment Report of the United Nations Intergovernmental Panel on Climate Change; NA =not applicable.

Source: Myhre et al. 2013.

tiple emissions models and is subject to the limitation of those models. The methods used to develop the CAMS emissions data set are described in Granier et al. (2019).

## GHG-2: Impact of trees on greenhouse gases

### DEFINITION

The average annual greenhouse gas net flux from trees (2001–21) per hectare (ha) of city area (megagrams [Mg] CO<sub>2</sub>e/ha).

### IMPORTANCE

Trees are critical contributors to a balanced climate system. Whereas healthy, growing trees remove carbon from the atmosphere and sequester it, trees that are cut or die emit carbon (Gibbs et al. 2022). Cities can work to keep forests and trees healthy and invest in expanding tree cover locally, regionally, and globally to increase carbon removals and reduce their contributions to climate change (Pool et al. 2022; Wilson et al. 2022).

### METHODS

This indicator is calculated from the Net Carbon Flux from Forests data set (Version 1.2.2) per Harris et al. (2021), as accessed on Google Earth Engine.<sup>18</sup> This 30 m resolution data layer provides an estimate of net carbon flux from trees (gross emissions minus gross removals) from 2001 through 2021 inclusive in units of Mg CO<sub>2</sub>e/ha. To calculate the mean annual carbon flux for each area of interest, we first unmask the data

set; then pixels where the data set shows no carbon flux are given a value of zero and are included in subsequent calculations. Next, we calculate the mean for the area and divide the resulting value by 21 to annualize the 21-year data set. The resulting value estimates the average carbon net flux per hectare from the area of interest during each year in the 21-year period. As we are interested in measuring city and area characteristics based on their full geographies, not just forest areas, net flux was normalized using total area as the denominator.

Negative numbers represent net greenhouse gas removals, and positive values indicate net emissions.

### LIMITATIONS

The carbon flux model used for the calculations was designed for forests and is based on tree cover as detected by Landsat, which means it does not pick up or measure carbon flux from sparse tree cover. At 30 m resolution, Landsat and products developed from it do not pick up isolated trees. Additionally, the model is limited to pixels with tree canopy density greater than 30 percent and trees of less than 5 m height in 2000 or subsequent tree cover gain, so low density or short tree cover is not included. Other limitations of the net flux data are described in Harris et al. (2021).

This indicator does not measure the impacts of indirect land-use change or the greenhouse gas implications of land-use decisions outside its borders. For instance, if a city chooses to avoid devel-

oping a green area within its borders, this may lead to exporting the development to nearby suburban areas, possibly resulting in the loss of a greater number of trees and increased transportation demand, both of which could increase net carbon emissions. When making decisions related to land use, cities should consider both the direct and indirect impacts of those decisions.

## Heat (HEA)

Due to the urban heat island effect, cities and their residents are exposed to greater heat hazard than equivalent rural areas. Climate change is expected to further exacerbate this risk to cities. These indicators measure local heat hazard and the presence of heat-mitigating infrastructure.

### HEA-1: Extreme heat hazard

#### DEFINITION

The expected extreme heat event hazard (expected days above 35°C in 2050) and trend (percentage change between 2020 and 2050 in number of days exceeding a threshold of 35°C).

#### IMPORTANCE

Understanding the hazard presented by extreme heat and the likely future change of that hazard can inform planning for an extreme heat event and investing in infrastructure that can help mitigate its impacts. The temperature at which heat is “extreme” depends on location and on the potential impacts at issue.

#### METHODS

This indicator is calculated as

$$\frac{x_{2050} - x_{2020}}{x_{2020}} \times 100$$

where  $x_{year}$  is the expected number of days in which the maximum near-surface air temperature is above 35°C in *year*. This value is calculated from a probability distribution modeled using ERA5 reanalysis historical temperature data (Hersbach et al. 2020) and NEX-GDDP ensemble climate projections (Thrasher et al. 2012). In our implementation, the indicator is processed for the 0.25-degree pixel containing the city centroid. Because of the coarse resolution of this data set, we only report value for the geographic area of the full city and not for each subcity area. We chose the years 2020 and 2050 to span a large number of years while still remaining in the time horizon of interest to many target users. We chose 35°C as an extreme-heat threshold; in high humidity, 35°C is likely to be lethal for human beings (Asseng et al. 2021).

More detailed documentation of these methods is under development, and we plan to publish it in a future technical note.

#### LIMITATIONS

This indicator is based on estimates of precipitation magnitude probabilities as modeled by climate simulations. There are unavoidable errors from numerous sources, including climate stochasticity, scientific uncertainty regarding Earth system processes, and uncertainty in future greenhouse gas emissions trends. Notably, we use the expected value of a random variable as a way to capture information about a probability distribution in a single number. It should not be interpreted as a prediction.

The 35°C threshold is not the only temperature that could be useful for calculating this indicator. For example, 30°C is established as being associated with significant decreases in human health and productivity (Tuholske et al. 2021). Users implementing this indicator would be wise to consult public health officials to identify a locally appropriate temperature threshold.

The 30°C and 35°C thresholds have both been studied as a wet-bulb globe temperature—that is, they are believed to be dangerous at high enough humidity that evaporation cannot cool a body below them. Due to lack of humidity variables in Coupled Model Intercomparison Project Phase 5 (CMIP5) data used in NEX-GDDP, our current implementation does not account for humidity and does not calculate a wet-bulb globe temperature, but future implementations will.

### HEA-2: Land surface temperature

#### DEFINITION

The percentage of built land with a high land surface temperature (LST) during the hot season (greater than or equal to 3°C above mean for built land).

#### IMPORTANCE

LST is closely correlated with near-surface air temperature, which is how people experience heat. This metric can identify areas of the city exposed to above-average heat. Such areas may be good candidates for heat mitigation measures such as increased tree or vegetation cover or solar reflective surfaces.

#### METHODS

This indicator uses LST for each pixel in the area of interest calculated using the methods from Ermida et al. (2020) and Landsat imagery, at 30 m resolution, as retrieved from Google Earth Engine. Mean LST is calculated from a mosaic of cloud-masked Landsat images from 2013 to 2022 selected from the month of the year that had the hottest day during this period

as determined from the ERA5 daily aggregates (Hersbach et al. 2020). Average and pixel-wise LST is then retrieved for built land cover areas using the built-up class from the ESA WorldCover as a mask. Finally, areas that are 3°C or more above the area average are masked to calculate the percentage of built area with high LST.

### LIMITATIONS

These calculations are based entirely on remotely sensed data, which are not assessed against local ground truth data. Notably, LST is not a direct measure of how people in cities experience heat, which is more closely related to near-surface air temperature and heat indices. Additionally, this indicator uses measurements from the times of day at which Landsat retrieves images, usually within a few hours of midday locally. As a result, this indicator does not measure heat in the evening or at night, which is important for understanding local heat impacts. Finally, because this indicator uses an image mosaic to remove cloud cover and provide an average for the hot season in the location, it does not reflect any one year, day, or heat event.

## HEA-3: Surface reflectivity

### DEFINITION

The percentage of built land with low surface reflectivity (below 0.2 albedo).

### IMPORTANCE

This indicator can identify areas of the city with a high share of surfaces that retain excess heat. Surfaces with low solar reflectivity (albedo) absorb heat and transfer it to immediate surroundings. Areas with a high share of low albedo surfaces may be candidates for installing measures—such as trees or solar reflective roofs and pavements—that will reduce the heat retained on surfaces or otherwise cool the immediate area.

### METHODS

This indicator uses pixel-wise albedo values derived from Sentinel-2, at 10 m resolution, as retrieved from Google Earth Engine using the algorithms defined by Bonafoni and Sekertekin (2020). Annual mean albedo is calculated from cloud-free pixels from 2021. Values for built land cover areas only are derived using the built-up class from the 10 m resolution ESA WorldCover data set as a mask. Finally, pixels with albedo values below 0.2—a common threshold used for defining moderately reflective surfaces (Energy Star n.d.)—are masked to calculate the percentage of built area with low surface reflectivity.

### LIMITATIONS

These calculations are based fully on remotely sensed data, which are subject to atmospheric interference and other challenges in data collection and are not assessed against local ground truth data. This indicator uses an image mosaic to remove cloud cover and provide an annual average; thus, it does not reflect the situation at any one point in time.

## HEA-4: Built land without tree cover

### DEFINITION

The percentage of built land without tree cover.

### IMPORTANCE

This indicator can identify city areas without significant tree cover and therefore lacking in shade and evapotranspiration that can reduce local heat. Tree cover in built areas varies significantly across cities. Tree cover can provide a cooling effect, documented to be in the range of 3°C (Wang et al. 2018), in urban areas. Areas without tree cover are often exposed to a higher extreme heat hazard. Areas with low tree cover may be candidates for implementing heat mitigation measures—such as trees, other vegetation, or solar reflective roofs and pavements—that will reduce the heat retained locally or otherwise cool the immediate area.

### METHODS

This indicator uses 10 m resolution tree cover data for 2020 from the Trees in Mosaic Landscapes data set (Brandt et al. 2022), which gives tree extent within each 10 m pixel, as retrieved from Google Earth Engine. The built-up class for 2020 from ESA WorldCover is used to mask the tree cover layer. The number of built pixels with tree cover is counted, all built pixels are counted, and these two values are divided to calculate the percentage of built land with tree cover. This value for percent tree cover is then inverted to derive a value for the percentage of built-up land without tree cover.

### LIMITATIONS

The limitations associated with data from Brandt et al. (2022), as described in ACC-4, also apply to this indicator.

## Land protection and restoration (LND)

Cities play an important role in protecting and restoring natural lands. These lands provide ecosystem services to cities, habitat to wildlife, and other benefits. These indicators classify and measure the characteristics of land within the city or track changes over time.

---

## LND-1: Permeable areas

### DEFINITION

The percentage of land area that has a permeable (pervious) surface.

### IMPORTANCE

Impervious areas are areas in which pavement or other surfaces prevent water from infiltrating the soil. As climate change in many places will change precipitation regimes, many cities with large areas of impervious surfaces will experience high peaks in water runoff, resulting stormwater flooding, and damage to infrastructure and natural areas. This type of flooding also lowers the quality of receiving waters fed by surface water runoff, impacting the water quality for the biodiversity of aquatic and marine systems downstream.

### METHODS

This indicator is calculated by measuring the proportion of all permeable areas to total terrestrial area of city:

$$\frac{\text{total permeable area}}{\text{total area of city}}$$

Permeable areas are taken from the Global Artificial Impervious Area (GAIA) impervious surface data set (Gong et al. 2020), which classifies land at a 30 m spatial resolution as permeable or impermeable to water based on vegetation dynamics, water content, and reflectance. Water bodies and undeveloped land are assumed to be permeable. This indicator is similar to FLD-4, with two distinctions: it considers all land in the area of interest (not just built-up land), and the numerator in the calculation is permeable area (not impermeable area).

### LIMITATIONS

These calculations are based entirely on remotely sensed data, which are not assessed against local ground truth data. Other variables that factor into permeability that are not detectable with remote sensing (such as soil type) are not considered in this analysis.

## LND-2: Tree cover

### DEFINITION

The percentage of land area that has tree cover.

### IMPORTANCE

Trees provide numerous services to cities. They provide cooling, improve air quality, store carbon, reduce noise pollution, and regulate the water cycle. Trees also provide habitat for birds, insects, and mammals, and they generally improve local ecosystem health (Wilson et al. 2022).

### METHODS

This indicator uses 10 m resolution tree cover data for 2020 from the Trees in Mosaic Landscapes data set (Brandt et al. 2022) as retrieved from Google Earth Engine, which gives the percentage of tree cover for each 10 m pixel. The formula used is as follows:

$$\frac{\text{area with tree cover}}{\text{total area of city}}$$

This indicator differs from indicator HEA-4 in three ways: it calculates the mean tree cover of all relevant pixels (rather than the percentage of pixels with any tree cover), it is calculated over the entire area of interest (not just built-up areas within it), and it counts the areas with tree cover (rather than those without).

### LIMITATIONS

The limitations associated with data from Brandt et al. (2022), as described in ACC-4, also apply to this indicator.

## LND-3: Change in vegetation and water cover

### DEFINITION

The net increase or decrease in area of vegetation and water cover between 2019 and 2022 as a percentage of the area with vegetation and water cover in 2019.

### IMPORTANCE

Vegetation and water cover provide many ecosystem services to cities, including groundwater recharge, flood management, and temperature moderation. They also provide critical prerequisites to habitat for wildlife.

## METHODS

This indicator uses a trend line of the measurements of remote sensing spectral indices from 2019 to 2022 to estimate the change in the presence of vegetation and water at points within each city. We use 10 m Sentinel-2 data, as accessed on Google Earth Engine and cloud masked (ESA 2015a), to calculate spectral indices associated with vegetation (NDVI) and water (NDWI). We then create annual greenest/bluest pixel mosaics for each year. We calculate trend lines of greenness and blueness for each pixel over the four-year period, filter to pixels with trend lines that are significant to a P value of 0.05, and flag pixels with an average annual change (slope) of at least (+/-)0.1 in its index value. Although some studies use much lower slope values to detect change (Forkel et al. 2013), we selected this comparatively high threshold slope value to restrict the results to obvious major changes related to likely changes in land use or environmental context (e.g., vegetation cleared for construction, a lake bed filled with water again after a major drought) rather than gradual changes (e.g., natural succession, crop rotation). We then mask these trend layers by layers that include all pixels that meet the threshold for vegetation (NDVI of at least 0.4) (EOS Data Analytics 2019) or water (NDWI of at least 0.3) in at least one study year so as to exclude pixels that are not likely to be vegetation or water in any year. Next, we separate these change layers into gain and loss layers (one with slope values greater than zero and another with values less than zero), combine the separate vegetation and water layers to produce one gain and one loss layer, and apply 30 m resolution reductions (using the mean trend line values of the 10 m pixels within a 30 m pixel) to count the number of pixels of loss and gain for either vegetation or water in each city and subcity area. We then subtract the loss pixels from the count of gain pixels to produce a net change in vegetation and water pixels. To normalize this value so it represents a percentage increase or decrease in vegetation and water area, we divide it by the total number of 30 m pixels that met the index value threshold for vegetation or water in 2019 for the same area of interest.

## LIMITATIONS

This indicator measures both change in the area of vegetation/water cover as well as change in the strength of the vegetation or water signal provided by the index. Most importantly, pixels classified as vegetation change include areas of gained (e.g., conversion from bare ground to green field) and lost vegetation (e.g., a forest converted to buildings) as well as changes to existing vegetation areas that have become observably greener (e.g., a meadow that is growing tree cover due to succession) or less green (e.g., an existing field that is now used to grow a differ-

ent crop). Not all vegetation or water provides equal benefits. These varying characteristics of green and blue features are not measured with this method.

## LND-4: Habitat areas restored

### DEFINITION

The area of habitat land restored between 2000 and 2020 as a percentage of habitat land in 2000.

### IMPORTANCE

Cities can directly improve biodiversity by converting poor habitat or nonhabitat land to good habitat. Good habitat generally includes multispecies vegetation and enough structural complexity to provide shade and cover from predators. The Singapore Index's Indicator 7 calls on cities either to estimate the area of land restored to "good ecological functioning" or to enumerate the types of habitat restored. This indicator supports the area of land restored method.

### METHODS

We are unable to discern habitat quality using global data, but we can provide data on changes in land classification from nonhabitat to habitat. We used the Landsat Analysis Ready Data (Potapov et al. 2022) from the Global Land Analysis and Discovery research group at the University of Maryland.<sup>19</sup> We defined habitat as aquatic or noncropland vegetated classes, and we compared classifications from 2000 and 2020. We defined new habitat as pixels that were classified as nonhabitat (urban, cropland, or bare) in 2000 but as habitat in 2020. For this indicator, we calculated

$$\frac{\text{area of habitat in 2020} - \text{area of habitat in 2000}}{\text{area of nonhabitat in 2000}}$$

### LIMITATIONS

This method differs somewhat from what is described in the Singapore Index's Indicator 7. Our denominator is nonhabitat rather than degraded habitat. Our estimate probably underestimates restoration as measured by this indicator.

---

## LND-5: Habitat types restored

### DEFINITION

The number of habitat types restored between 2000 and 2020 as a percentage of all habitat types in the area.

### IMPORTANCE

Cities can directly improve biodiversity by converting poor habitat or nonhabitat land to good habitat. Good habitat generally includes multispecies vegetation and enough structural complexity to provide shade and cover. The Singapore Index's Indicator 7 calls on cities either to estimate the area of land restored to "good ecological functioning" or to enumerate the types of habitat restored. This indicator supports the habitat-type enumeration method.

### METHODS

This indicator is calculated by the formula

$$\frac{\text{number of habitat types restored}}{\text{number of habitat types in city in baseline year}}$$

The Landsat Analysis Ready Data discerns six land cover classes that we include as types of habitat: short vegetation, forest, tall forest (taller than 20 m), wetland with short vegetation, wetland forest, and open water. (We treated the classes for bare ground, snow or ice, cropland, and built-up area as nonhabitat.) We calculate our indicator by identifying areas of new habitat, where habitat existed in 2020 but not in 2000; counting the number of habitat types (i.e., aquatic and vegetated land cover classes) in these areas of new habitat; and comparing this number to the total number of habitat types in the city in 2020. For example, consider a city that had four types of habitat in 2020. We look for all habitat areas in 2020 that were nonhabitat in the baseline year 2000 and consider these to be new habitat areas. If there are two habitat types in the new habitat areas, then the indicator is as follows:

$$\frac{2 \text{ habitat types in new habitat}}{4 \text{ habitat types in city in 2020}} \times 100\% = 50\%$$

### LIMITATIONS

This indicator describes restoration as a fraction of the existing diversity of habitat types, not as the absolute diversity of restored habitat. It does not distinguish between a city that restores many

types of habitat and a city that simply has few habitat types. For example, in a city with six habitat types, restoration of six types of habitat will result in an indicator value of 100 percent. The indicator is also 100 percent if a city with just one habitat type restores just one habitat type. By scaling restored diversity by overall diversity, this indicator focuses narrowly on cities' efforts to restore native diversity and not on the diversity itself.

Our method also differs from that in the Singapore Index: we use new habitat instead of habitat that has been improved from degraded to good ecological function. Cities that have access to local data specifically detailing the extent and status of habitat restoration projects would probably benefit from calculating the Singapore Index's Indicator 7 using that data.

## LND-6: Protected areas

### DEFINITION

The percentage of land area that is designated as protected area.

### IMPORTANCE

Protected or secured natural areas indicate a government's legally formalized commitment to conserve biodiversity. Protected areas are lands (or waters) with legal restrictions on development or use and sometimes physical barriers to entry. Protected areas inside and near cities, including outside their jurisdictional boundaries, can provide multiple benefits to people living in cities in the form of human health and well-being and water security (Wilson et al. 2022). Importantly, they serve as havens for biodiversity and can be used to create ecological connectivity and restore previously lost biodiversity in the cityscape.

### METHODS

This indicator uses the following formula:

$$\frac{\text{area of protected or secured natural areas within city}}{\text{total area of city}}$$

Our data on protected areas come from the World Database on Protected Areas (WDPA), which is a collection of data on protected areas contributed by national governments (UNEP-WCMC and IUCN n.d.).

## LIMITATIONS

- This indicator measures only protected areas within city boundaries, excluding nearby protected areas.
- The WDPA is based on information contributed by national governments. It might exclude areas whose protections do not fit criteria set by these governments.
- Intensive, biodiversity-harming activities can occur within formally protected areas. We do not assess specific legal protections; nor do we assess enforcement of protections.

## LND-7: Protection of Key Biodiversity Areas

### DEFINITION

The percentage of Key Biodiversity Area (KBA) land that is designated as protected area.

### IMPORTANCE

KBAs are areas that have been identified by the KBA Partnership as being important to global biodiversity, generally because they include either a globally important type of habitat or because they include habitat for a globally important species (BirdLife International 2022). Criteria for inclusion include the presence of threatened biodiversity, the presence of geographically restricted biodiversity, ecological integrity, critical biological processes, and irreplaceability. Cities can threaten or contribute to the global persistence of biodiversity through their development choices. Limiting development within KBAs or formally protecting land within KBAs can protect biodiversity in these areas.

In addition to the map of local KBAs, we provide two indicators related to these areas (LND-7 and LND-8). Neither indicator corresponds directly to an indicator in the Singapore Index.

### METHODS

KBAs can often benefit from formal protection (KBA Partnership 2017). In this indicator, we provide information on how much of a city's KBA is currently under formal protection. This is the formula:

$$\frac{\text{area of KBA within city under formal protection}}{\text{total area of KBA within city}}$$

KBA data are provided by (BirdLife International 2022) for the KBA Partnership, and data on protected areas come from the WDPA (UNEP-WCMC and IUCN n.d.).

## LIMITATIONS

This indicator shares the limitations of LND-6 arising from limitations in the WDPA. Both the WDPA and the KBA data are periodically updated. Users who use values of this indicator calculated by WRI or others should note whether they were based on the most recent versions of the input data.

The terms of use provided by the KBA Partnership do not allow us to share the source KBA data, but all data can be requested from BirdLife International. Similarly, the United Nations Environment Programme World Conservation Monitoring Centre and the International Union for Conservation of Nature do not allow us to share the source data on protected areas, but all data are available on the WDPA website (<https://www.protectedplanet.net>).

## LND-8: Built-up KBAs

### DEFINITION

The percentage of KBA land that is built up.

### IMPORTANCE

Land expansion from cities and other settlements poses a major threat to biodiversity (McDonald et al. 2018). Habitat quality in built-up areas tends to be lower than in natural areas. Habitat quality in KBAs might therefore be improved by habitat restoration efforts that convert built-up areas to natural ecosystem types.

### METHODS

We provide an indicator that describes how much of the KBA within the city is built up. The formula is as follows:

$$\frac{\text{built-up area within KBA within city}}{\text{total area of KBA within city}}$$

The data on built-up areas are from the 2020 ESA WorldCover. KBA data are provided by BirdLife International (2022) for the KBA Partnership.

## LIMITATIONS

The KBA data are periodically updated. Users who use values of this indicator calculated by WRI or others should note whether they were based on the most recent versions of the input data.

The terms of use provided by the KBA Partnership do not allow us to share the source data, but all data can be requested on its website (<https://www.keybiodiversityareas.org>).

## GENERAL LIMITATIONS

The indicators developed through these methods can provide numerous insights on variations within and between cities and changes over time. However, there are limitations to the value provided by these indicators, uncertainty regarding the resulting indicator values, and caveats to their meaning and potential applications that should be understood. In addition to the limitations specific to each indicator mentioned, there are also a few general limitations. We have addressed these concerns to the extent practical through how specific indicators are defined and presented, but these issues remain important for users of the indicators.

- **Boundaries and aggregations.** These methods primarily focus on providing a summary value of each area of interest for each indicator. Doing so helps to simplify a large amount of data, but it can also obscure nuance and important information. First, the areas of interest need to be meaningful. We use administrative areas because they are important boundaries of authority for decision-makers and are often used to aggregate other information. But different boundaries result in different indicator values. Other boundaries may be more relevant to a different set of stakeholders in the same city. Boundaries can change over time, making comparisons difficult. And for some topics, other kinds of boundaries may be more appropriate to generate meaningful insights (e.g., watershed boundaries for hydrology). Second, how boundaries are drawn and the characteristics of the areas within the boundaries can profoundly affect the results of data aggregations for the area of interest. As an example, if a park is equally split between two city wards, and they have similar vegetation coverage, the boundaries could obscure the significant vegetation differences within their respective residential areas due to averaging. If the park were classified as a separate area of interest, a vegetation cover indicator would more accurately characterize the differences between the two remaining residential areas. Third, the size of the areas of interest in comparison to the scale of the data sets used to calculate indicators can produce results that range from insightful to near meaningless. For example, assume a city has equally sized square districts of 1 km in each direction. A raster data set that is at a smaller scale would give useful information about the area within the district (but if it is much smaller in scale, such as 10 m, it may give too much information for an aggregate indicator to fully summarize, as we discuss further below). However, if the data set is of a larger scale, say 10 km, aggregations at the smaller district scale result in the same value for many districts, which likely does not reflect the reality on the ground and does not give any meaningful information for comparison between the districts.
- **Data uncertainty and incompleteness.** The data sources used to calculate the indicators themselves have significant limitations. The global-scale data sets from remote sensing or crowdsourcing used for our indicators are limited by what sensors can detect, their minimum mapping unit, and user contributions. They can give the impression of completeness while not being relevant at the scale of the desired analysis or can be missing important contextual details. We document limitations of specific data sets within the description of methods for each indicator. In contrast, local data pose their own problems, including being limited in scope, using local definitions that are often incompatible with data used elsewhere, introducing bias to an analysis, and often being difficult to access. The time required to collect and process local data makes it impossible to use local data for this project, which aims to calculate shared indicators for eventually hundreds of cities around the world. Ultimately, decisions about the most appropriate data for a local challenge need to be made by or with local stakeholders. For this reason, methods with flexible data input sources are critical. Our indicator methods can be adapted by our team or other researchers for use with similar alternative data sets, including from local sources, if a more appropriate one is developed or identified.
- **Comparability between indicators and data sets.** The differences between data sets—such as their scale or dates of acquisition—can make it complex to use multiple data sets together. We intend for multiple indicators to be shared with stakeholders; however, indicators within the same thematic areas, and even indicators themselves, may draw on information from various data sets. Within individual indicators, we often use multiple data sets together (e.g., a primary data set and another data set to mask the data to focus on land cover types of interest) to develop an indicator statistic. The best data sets for required variables may be available for different years, meaning some changes during that time period are ignored or misrepresented. Or they may be of different scales, meaning that issues of aggregation (as discussed previously) or precision (e.g., more trees being detectable at a 10 m scale than a 30 m scale) can mean that the data sets show different information in the same place.
- **Spatial observational data are not enough.** Our indicators almost exclusively identify the current physical states or changes to them in cities. This information can establish

trends; benchmark areas against each other; and help identify opportunities, diagnose problems, and spatially target interventions. However, the indicators alone are likely not sufficient to identify actions and set targets. Domain expertise and local knowledge to identify options and planning processes to determine objectives are required. Importantly, these indicators do not measure or attribute influences on physical changes, such as policies or infrastructure investment, or their effectiveness. To track progress toward physical goals, observational data is essential. To understand which actions are working well and which are falling short, other data and methods are required.

## FURTHER WORK

These indicator methods and their uses can be further refined and enhanced. Options identified so far include the following:

- Develop a standard indicator workflow and shared database. Consolidating variations on our core workflow and indicator sets that have been developed for multiple projects would make it easier to quickly calculate any set of indicators for any set of areas of interest.
    - Package the indicator workflow solution into an open-source framework (R or Python package) that can be easily reused and/or updated by external/internal contributors.
  - Offer guidance on developing new or revised indicators emphasizing designs that are fit for purpose and data set comparison and selection.
  - Develop additional indicators or adapt existing indicator methods into our calculation framework to allow for similar standard measurements on other urban themes relevant to city decision-makers or stakeholders.
  - Calculate indicators for additional cities and for other initiatives supporting cities on sustainable development.
  - Compare our indicator findings with socioeconomic data to explore relationships between indicators of urban equity and the presence of urban amenities/risk in multiple cities.
  - Create a process for vetting and validating new global or local data layers as they become available to potentially integrate with and improve existing indicator methods.
  - Compare computed indicators using global data with computations from available local data for validation and provide support to stakeholders for collecting local data as needed.
- Calculate indicator time series for some areas of interest, where appropriate multiyear input data layers are available and where relevant to indicators.
  - Improve integration of user feedback and needs into indicator prioritization, design, and development.
    - Connect more with potential users and stakeholders and define their profiles, statuses, data capacities, and needs.
    - Conduct user needs assessments to better understand how the proposed indicators may help our stakeholders in their decision-making processes and what additional indicators—or modifications of existing indicators—may be useful for users.
    - Map our indicators with potential city-level actions and how the proposed metrics may drive them.
    - Create focus groups or case studies of cities sharing feedback on the value and uses of the data and indicators.

---

## ENDNOTES

1. To learn about the Cities4Forests initiative, visit <https://cities4forests.com/>.
2. For information about the UrbanShift initiative, see <https://www.shiftcities.org/>.
3. For more information about the OSM database, see <https://www.openstreetmap.org/>.
4. Current methods are documented in two separate code repositories, one for each initiative with which the indicators are being piloted: Cities4Forests (<https://github.com/wri/cities-cities4forests-indicators>) and UrbanShift (<https://github.com/wri/cities-urbanshift/tree/main/baseline-indicators>).
5. The "built-up" land cover class of WorldCover 2020 is defined as "land covered by buildings, roads and other man-made structures such as railroads. Buildings include both residential and industrial building. Urban green (parks, sport facilities) is not included in this class" (ESA 2020b).
6. For more information about the Trees in Mosaic Landscapes data set, see <https://resourcewatch.org/data/explore/Trees-in-Mosaic-Landscapes>.
7. To learn more about the Global Anthropogenic Emissions data set, see <https://eccad3.sedoo.fr/metadata/479>; for CAMS, see <https://atmosphere.copernicus.eu/>; and for ECCAD, see <https://eccad.aeris-data.fr/>.
8. For more information about the CAMS Global Reanalysis EAC4 data set, visit <https://www.ecmwf.int/en/forecasts/dataset/cams-global-reanalysis>.
9. To learn more about the V5.GL.02 data set, see <https://sites.wustl.edu/acag/datasets/surface-pm2-5/#V5.GL.02>, and for the Atmospheric Composition Analysis Group, see <https://sites.wustl.edu/acag/>.
10. For more information about the Aqueduct Floods database, visit <https://www.wri.org/applications/aqueduct/floods>.
11. Additional information about the ERA5 reanalysis can be found on the Google Earth Engine Data Catalog, [https://developers.google.com/earth-engine/datasets/catalog/ECMWF\\_ERA5\\_DAILY](https://developers.google.com/earth-engine/datasets/catalog/ECMWF_ERA5_DAILY).
12. More information about the NEX-GDDP ensemble climate projections is available on the Google Earth Engine Data Catalog, [https://developers.google.com/earth-engine/datasets/catalog/NASA\\_NEX-GDDP](https://developers.google.com/earth-engine/datasets/catalog/NASA_NEX-GDDP).
13. For additional information about the Global 30 m Height Above the Nearest Drainage data set, see <https://gee-community-catalog.org/projects/hand/>.
14. For more information about the 2020 ESA WorldCover, visit [https://developers.google.com/earth-engine/datasets/catalog/ESA\\_WorldCover\\_v100](https://developers.google.com/earth-engine/datasets/catalog/ESA_WorldCover_v100).
15. For more information about the Tsinghua annual maps, see [https://developers.google.com/earth-engine/datasets/catalog/Tsinghua\\_FROM-GLC\\_GAIA\\_v10](https://developers.google.com/earth-engine/datasets/catalog/Tsinghua_FROM-GLC_GAIA_v10).
16. More information about the JRC Global Surface Water data set is available at [https://developers.google.com/earth-engine/datasets/catalog/JRC\\_GSW1\\_3\\_GlobalSurfaceWater](https://developers.google.com/earth-engine/datasets/catalog/JRC_GSW1_3_GlobalSurfaceWater).
17. For additional information about Sentinel-2 data, see [https://developers.google.com/earth-engine/datasets/catalog/COPERNICUS\\_S2](https://developers.google.com/earth-engine/datasets/catalog/COPERNICUS_S2).
18. To access the Net Carbon Flux from Forests data set, visit <https://code.earthengine.google.com/?asset=projects/wri-datalab/gfw-data-lake/net-flux-forest-extent-per-ha-v1-2-2-2001-2021/net-flux-global-forest-extent-per-ha-2001-2021>.
19. To learn more about the Global Land Analysis and Discovery research group, visit <https://glad.umd.edu/>.

## REFERENCES

- Asseng, S., D. Spänkuch, I.M. Hernandez-Ochoa, and J. Laporta. 2021. "The Upper Temperature Thresholds of Life." *Lancet Planetary Health* 5 (6): e378–85. [https://doi.org/10.1016/S2542-5196\(21\)00079-6](https://doi.org/10.1016/S2542-5196(21)00079-6).
- Avtar, R., R. Aggarwal, A. Kharrazi, P. Kumar, and T.A. Kurniawan. 2019. "Utilizing Geospatial Information to Implement SDGs and Monitor Their Progress." *Environmental Monitoring and Assessment* 192 (December): 35. <https://doi.org/10.1007/s10061-019-7996-9>.
- BirdLife International. 2022. (Database.) *World Database of Key Biodiversity Areas*. Key Biodiversity Areas Partnership. <https://www.keybiodiversityareas.org/>.
- Bocher, E., G. Petit, J. Bernard, and S. Palominos. 2018. "A Geoprocessing Framework to Compute Urban Indicators: The MApUCE Tools Chain." *Urban Climate* 24 (June): 153–74. <https://doi.org/10.1016/j.uclim.2018.01.008>.
- Boeing, G., C. Higgs, S. Liu, B. Giles-Corti, J.F. Sallis, E. Cerin, M. Lowe, et al. 2022. "Using Open Data and Open-Source Software to Develop Spatial Indicators of Urban Design and Transport Features for Achieving Healthy and Sustainable Cities." *Lancet Global Health* 10 (6): e907–18. [https://doi.org/10.1016/S2214-109X\(22\)00072-9](https://doi.org/10.1016/S2214-109X(22)00072-9).
- Bonafoni, S., and A. Sekertekin. 2020. "Albedo Retrieval from Sentinel-2 by New Narrow-to-Broadband Conversion Coefficients." *IEEE Geoscience and Remote Sensing Letters* 17 (9): 1618–22. <https://doi.org/10.1109/LGRS.2020.2967085>.
- Brandt, J., J. Ertel, J. Spore, and F. Stolle. 2022. "The Extent of Trees in the Tropics." Research Square, September 29. <https://doi.org/10.21203/rs.3.rs-2109093/v1>.
- Chan, L., O. Hillel, P. Werner, N. Holman, I. Coetzee, R. Galt, and T. Elmquist. 2021. "Handbook on the Singapore Index on Cities' Biodiversity (also Known as the City Biodiversity Index)." CBD Technical Series 98. Montreal: Secretariat of the Convention on Biological Diversity; Singapore: National Parks Board. <https://www.cbd.int/doc/publications/cbd-ts-98-en.pdf>.
- Cochran, F., J. Daniel, L. Jackson, and A. Neale. 2020. "Earth Observation-Based Ecosystem Services Indicators for National and Sub-national Reporting of the Sustainable Development Goals." *Remote Sensing of Environment* 244 (July): 111796. <https://doi.org/10.1016/j.rse.2020.111796>.
- Croke, J., C. Thompson, and K. Fryirs. 2017. "Prioritising the Placement of Riparian Vegetation to Reduce Flood Risk and End-of-Catchment Sediment Yields: Important Considerations in Hydrologically-Variable Regions." *Journal of Environmental Management* 190 (April): 9–19. <https://doi.org/10.1016/j.jenvman.2016.12.046>.
- Deslauriers, M.R., A. Asgary, N. Nazarnia, and J.A.G. Jaeger. 2018. "Implementing the Connectivity of Natural Areas in Cities as an Indicator in the City Biodiversity Index (CBI)," in "Landscape Indicators—Monitoring of Biodiversity and Ecosystem Services at Landscape Level," edited by U. Walz and R.-U. Syrbe, special issue, *Ecological Indicators* 94 (November): 99–113. <https://doi.org/10.1016/j.ecolind.2017.02.028>.
- Donchyts, G., H. Winsemius, J. Schellekens, T. Erickson, H. Gao, H. Savenije, and N. van de Giesen. 2016. "Global 30m Height above the Nearest Drainage (HAND)." *Geophysical Research Abstracts* 18: EGU2016-17445-3. <https://gee-community-catalog.org/projects/hand/>.
- Energy Star. n.d. "ENERGY STAR Program Requirements for Roof Products: Partner Commitments." [https://www.energystar.gov/sites/default/files/specs//Roof%20Products%20V3%20Program%20Requirements\\_0.pdf](https://www.energystar.gov/sites/default/files/specs//Roof%20Products%20V3%20Program%20Requirements_0.pdf). Accessed March 7, 2023.
- Engel-Cox, J.A., R.M. Hoff, and A.D.J. Haymet. 2004. "Recommendations on the Use of Satellite Remote-Sensing Data for Urban Air Quality." *Journal of the Air & Waste Management Association* 54 (11): 1360–71. <https://doi.org/10.1080/10473289.2004.10471005>.
- EOS Data Analytics. 2019. "NDVI FAQ: All You Need to Know about Index." *Agriculture* (blog), August 30. <https://eos.com/blog/ndvi-faq-all-you-need-to-know-about-ndvi/>.
- EPA (U.S. Environmental Protection Agency). n.d. "Understanding Global Warming Potentials." <https://www.epa.gov/ghgemissions/understanding-global-warming-potentials>. Accessed January 12, 2016.

- Ermida, S.L., P. Soares, V. Mantas, F.-M. Götsche, and I.F. Trigo. 2020. "Google Earth Engine Open-Source Code for Land Surface Temperature Estimation from the Landsat Series." *Remote Sensing* 12 (9): 1471. <https://doi.org/10.3390/rs12091471>.
- ESA (European Space Agency). 2015a. "Sentinel-2: Cloud Probability." Earth Engine Data Catalog. [https://developers.google.com/earth-engine/datasets/catalog/COPERNICUS\\_S2\\_CLOUD\\_PROBABILITY](https://developers.google.com/earth-engine/datasets/catalog/COPERNICUS_S2_CLOUD_PROBABILITY).
- ESA. 2015b. "Sentinel-2 MSI: MultiSpectral Instrument, Level-1C." Earth Engine Data Catalog. [https://developers.google.com/earth-engine/datasets/catalog/COPERNICUS\\_S2](https://developers.google.com/earth-engine/datasets/catalog/COPERNICUS_S2).
- ESA. 2020a. "ESA WorldCover 10m V100." Earth Engine Data Catalog. [https://developers.google.com/earth-engine/datasets/catalog/ESA\\_WorldCover\\_v100](https://developers.google.com/earth-engine/datasets/catalog/ESA_WorldCover_v100).
- ESA. 2020b. *WorldCover Product User Manual, Version 1.0*. Paris: ESA. [https://worldcover2020.esa.int/data/docs/WorldCover\\_PUM\\_V1.1.pdf](https://worldcover2020.esa.int/data/docs/WorldCover_PUM_V1.1.pdf).
- Fahrig, L. 2003. "Effects of Habitat Fragmentation on Biodiversity." *Annual Review of Ecology, Evolution, and Systematics* 34: 487–515. <https://doi.org/10.1146/annurev.ecolsys.34.011802.132419>.
- Feng, S., D. Gao, F. Liao, F. Zhou, and X. Wang. 2016. "The Health Effects of Ambient PM<sub>2.5</sub> and Potential Mechanisms." *Ecotoxicology and Environmental Safety* 128 (June): 67–74. <https://doi.org/10.1016/j.ecoenv.2016.01.030>.
- Forkel, M., N. Carvalhais, J. Verbesselt, M.D. Mahecha, C.S.R. Neigh, and M. Reichstein. 2013. "Trend Change Detection in NDVI Time Series: Effects of Inter-annual Variability and Methodology." *Remote Sensing* 5 (5): 2113–44. <https://doi.org/10.3390/rs5052113>.
- Forman, R.T.T., and M. Godron. 1991. *Landscape Ecology*. Hoboken, NJ: Wiley. <https://www.wiley.com/en-us/Landscape+Ecology-p-9780471870371>.
- Fritz, S., L. See, T. Carlson, M. Haklay, J.L. Oliver, D. Fraisl, R. Mondardini, et al. 2019. "Citizen Science and the United Nations Sustainable Development Goals." *Nature Sustainability* 2 (October): 922–30. <https://doi.org/10.1038/s41893-019-0390-3>.
- GBIF (Global Biodiversity Information Facility). 2022a. "Occurrence Download—Arthropods." <https://doi.org/10.15468/DL.DWV9AP>.
- GBIF. 2022b. "Occurrence Download—Birds." <https://doi.org/10.15468/DL.H4AZRE>.
- GBIF. 2022c. "Occurrence Download—Vascular Plants." <https://doi.org/10.15468/DL.6WANKS>.
- Geemap. n.d. "OSM Module." <https://geemap.org/osm/>. Accessed November 8, 2022.
- Gibbs, D., N. Harris, and J.-R. Pool. 2022. *Global Protocol for Community-Scale Greenhouse Gas Inventories: Supplemental Guidance for Forests and Trees*. Washington, DC: Greenhouse Gas Protocol, World Resources Institute. <https://ghgprotocol.org/gpc-supplemental-guidance-forests-and-trees>.
- Giuliani, G., E. Petri, E. Interwies, V. Vysna, Y. Guigoz, N. Ray, and I. Dickie. 2021. "Modelling Accessibility to Urban Green Areas Using Open Earth Observations Data: A Novel Approach to Support the Urban SDG in Four European Cities." *Remote Sensing* 13 (3): 422. <https://doi.org/10.3390/rs13030422>.
- Gong, P., X. Li, J. Wang, Y. Bai, B. Chen, T. Hu, X. Liu, et al. 2020. "Annual Maps of Global Artificial Impervious Area (GAIA) between 1985 and 2018." *Remote Sensing of Environment* 236 (January): 111510. <https://doi.org/10.1016/j.rse.2019.111510>.
- GEE (Google Earth Engine). 2021. "Weighted Reductions." May 27. [https://developers.google.com/earth-engine/guides/reducers\\_weighting](https://developers.google.com/earth-engine/guides/reducers_weighting). Accessed November 8, 2022.
- GEE. 2022. "Ee.Terrain.slope." August 1. <https://developers.google.com/earth-engine/apidocs/ee-terrain-slope>.
- Granier, C., S. Darras, H. Denier van der Gon, J. Doubalova, N. Elguindi, B. Galle, M. Gauss, et al. 2019. "The Copernicus Atmosphere Monitoring Service Global and Regional Emissions (April 2019 Version)." Copernicus Atmosphere Monitoring Service. <https://doi.org/10.24380/DOBN-KX16>.
- Harris, N.L., D.A. Gibbs, A. Baccini, R.A. Birdsey, S. de Bruin, M. Farina, L. Fatoyinbo, et al. 2021. "Global Maps of Twenty-First Century Forest Carbon Fluxes." *Nature Climate Change* 11 (3): 234–40. <https://doi.org/10.1038/s41558-020-00976-6>.

- Helmrich, A.M., B.L. Ruddell, K. Bessem, M.V. Chester, N. Chohan, E. Doerry, J. Eppinger, et al. 2021. "Opportunities for Crowdsourcing in Urban Flood Monitoring." *Environmental Modelling & Software* 143 (September): 105124. <https://doi.org/10.1016/j.envsoft.2021.105124>.
- Hersbach, H., B. Bell, P. Berrisford, S. Hirahara, A. Horányi, J. Muñoz-Sabater, J. Nicolas, et al. 2020. "The ERA5 Global Reanalysis." *Quarterly Journal of the Royal Meteorological Society* 146 (730): 1999–2049. <https://doi.org/10.1002/qj.3803>.
- Inness, A., M. Ades, A. Agustí-Panaredaz, J. Barré, A. Benedictow, A. Blechschmidt, J. Dominguez, et al. 2019. "CAMS Global Reanalysis (EAC4)." Copernicus Atmosphere Monitoring Service. <https://ads.atmosphere.copernicus.eu/cdsapp#!/dataset/cams-global-reanalysis-eac4?tab=overview>.
- Jing, C., M. Du, S. Li, and S. Liu. 2019. "Geospatial Dashboards for Monitoring Smart City Performance." *Sustainability* 11 (20): 5648. <https://doi.org/10.3390/su11205648>.
- Kalluri, S., P. Gilruth, and R. Bergman. 2003. "The Potential of Remote Sensing Data for Decision Makers at the State, Local and Tribal Level: Experiences from NASA's Synergy Program." *Environmental Science & Policy* 6 (6): 487–500. <https://doi.org/10.1016/j.envsci.2003.08.002>.
- Kampa, M., and E. Castanas. 2008. "Human Health Effects of Air Pollution." *Environmental Pollution* 151 (2): 362–67. <https://doi.org/10.1016/j.envpol.2007.06.012>.
- Kavvada, A., G. Metternicht, F. Kerblat, N. Mudau, M. Haldorson, S. Laldaparsad, L. Friedl, A. Held, and E. Chuvieco. 2020. "Towards Delivering on the Sustainable Development Goals Using Earth Observations." *Remote Sensing of Environment* 247 (September): 111930. <https://doi.org/10.1016/j.rse.2020.111930>.
- KBA (Key Biodiversity Areas) Partnership. 2017. *The Relationship between Key Biodiversity Areas (KBAs) and Protected Areas*. Cambridge, UK: KBA Secretariat, Birdlife International. <https://www.keybiodiversityareas.org/assets/8f1535aed3316ae2b720364019f8cb1c>.
- Kondo, M.C., S. Han, G.H. Donovan, and J.M. MacDonald. 2017. "The Association between Urban Trees and Crime: Evidence from the Spread of the Emerald Ash Borer in Cincinnati." *Landscape and Urban Planning* 157 (January): 193–99. <https://doi.org/10.1016/j.landurbplan.2016.07.003>.
- Kuffer, M., J. Wang, M. Nagenborg, K. Pfeffer, D. Kohli, R. Sliuzas, and C. Persello. 2018. "The Scope of Earth-Observation to Improve the Consistency of the SDG Slum Indicator." *ISPRS International Journal of Geo-Information* 7 (11): 428. <https://doi.org/10.3390/ijgi7110428>.
- Kuffer, M., D.R. Thomson, G. Boo, R. Mahabir, T. Grippa, S. Vanhuysse, R. Engstrom, et al. 2020. "The Role of Earth Observation in an Integrated Deprived Area Mapping 'System' for Low-to-Middle Income Countries." *Remote Sensing* 12 (6): 982. <https://doi.org/10.3390/rs12060982>.
- Lee, K.K., M.R. Miller, and A.S.V. Shah. 2018. "Air Pollution and Stroke." *Journal of Stroke* 20 (1): 2–11. <https://doi.org/10.5853/jos.2017.02894>.
- Lind, L., E.M. Hasselquist, and H. Laudon. 2019. "Towards Ecologically Functional Riparian Zones: A Meta-analysis to Develop Guidelines for Protecting Ecosystem Functions and Biodiversity in Agricultural Landscapes." *Journal of Environmental Management* 249 (November): 109391. <https://doi.org/10.1016/j.jenvman.2019.109391>.
- Litwiller, F., C. White, K. Gallant, S. Hutchinson, and B. Hamilton-Hinch. 2016. "Recreation for Mental Health Recovery." *Leisure/Loisir* 40 (3): 345–65. <https://doi.org/10.1080/14927713.2016.1252940>.
- Ludwig, C., R. Hecht, S. Lautenbach, M. Schorcht, and A. Zipf. 2021. "Mapping Public Urban Green Spaces Based on OpenStreetMap and Sentinel-2 Imagery Using Belief Functions." *ISPRS International Journal of Geo-Information* 10 (4): 251. <https://doi.org/10.3390/ijgi10040251>.
- Martinuzzi, S., O.M. Ramos-González, T.A. Muñoz-Erickson, D.H. Locke, A.E. Lugo, and V.C. Radeloff. 2018. "Vegetation Cover in Relation to Socioeconomic Factors in a Tropical City Assessed from Sub-meter Resolution Imagery." *Ecological Applications* 28 (3): 681–93. <https://doi.org/10.1002/eap.1673>.
- Martinuzzi, S., D.H. Locke, O. Ramos-González, M. Sanchez, J.M. Grove, T.A. Muñoz-Erickson, W.J. Arendt, and G. Bauer. 2021. "Exploring the Relationships between Tree Canopy Cover and Socioeconomic Characteristics in Tropical Urban Systems: The Case of Santo Domingo, Dominican Republic." *Urban Forestry & Urban Greening* 62 (July): 127125. <https://doi.org/10.1016/j.ufug.2021.127125>.

- McDonald, R.I., M. Colbert, M. Hamann, R. Simkin, and B. Walsh. 2018. *Nature in the Urban Century: A Global Assessment of Where and How to Conserve Nature for Biodiversity and Human Wellbeing*. Arlington County, VA: The Nature Conservancy. <https://www.nature.org/en-us/what-we-do/our-insights/perspectives/nature-in-the-urban-century/>.
- McFeeters, S.K. 2013. "Using the Normalized Difference Water Index (NDWI) within a Geographic Information System to Detect Swimming Pools for Mosquito Abatement: A Practical Approach." *Remote Sensing* 5 (7): 3544–61. <https://doi.org/10.3390/rs5073544>.
- Myhre, G., D. Shindell, F.-M. Bréon, W. Collins, J. Fuglestedt, J. Huang, D. Koch, et al. 2013. "Anthropogenic and Natural Radiative Forcing." In *Climate Change 2013: The Physical Science Basis*. Contribution of Working Group I to the Fifth Assessment Report of the Intergovernmental Panel on Climate Change, edited by T.F. Stocker, D. Qin, G.-K. Plattner, M. Tignor, S.K. Allen, J. Boschung, A. Nauels, Y. Xia, V. Bex, and P.M. Midgley, 659–740. Cambridge and New York: Cambridge University Press. [https://www.ipcc.ch/site/assets/uploads/2018/02/WG1AR5\\_Chapter08\\_FINAL.pdf](https://www.ipcc.ch/site/assets/uploads/2018/02/WG1AR5_Chapter08_FINAL.pdf).
- NASA JPL (National Aeronautics and Space Administration Jet Propulsion Laboratory). 2020. "NASADEM Merged DEM Global 1 Arc Second V001." Earth Engine Data Catalog. [https://developers.google.com/earth-engine/datasets/catalog/NASA\\_NASADEM\\_HGT\\_001](https://developers.google.com/earth-engine/datasets/catalog/NASA_NASADEM_HGT_001).
- Nicoletti, L., M. Sirenko, and T. Verma. 2022. "Disadvantaged Communities Have Lower Access to Urban Infrastructure." *Environment and Planning B: Urban Analytics and City Science*, October. <https://doi.org/10.1177/23998083221131044>.
- Niu, H., and E.A. Silva. 2020. "Crowdsourced Data Mining for Urban Activity: Review of Data Sources, Applications, and Methods." *Journal of Urban Planning and Development* 146 (2): 04020007. [https://doi.org/10.1061/\(ASCE\)UP.1943-5444.0000566](https://doi.org/10.1061/(ASCE)UP.1943-5444.0000566).
- Pekel, J.-F., A. Cottam, N. Gorelick, and A.S. Belward. 2016. "High-Resolution Mapping of Global Surface Water and Its Long-Term Changes." *Nature* 540 (December): 418–22. <https://doi.org/10.1038/nature20584>.
- Pietilä, M., M. Neuvonen, K. Borodulin, K. Korpela, T. Sievänen, and L. Tyrväinen. 2015. "Relationships between Exposure to Urban Green Spaces, Physical Activity and Self-Rated Health." *Journal of Outdoor Recreation and Tourism* 10 (July): 44–54. <https://doi.org/10.1016/j.jort.2015.06.006>.
- Pool, J.-R., D. Gibbs, S. Alexander, and N. Harris. 2022. "5 Reasons Cities Should Include Trees in Climate Action." *Insights* (blog), July 28. <https://www.wri.org/insights/urban-trees-city-climate-action>.
- Potapov, P., M.C. Hansen, A. Pickens, A. Hernandez-Serna, A. Tyukavina, S. Turubanova, V. Zalles, et al. 2022. "The Global 2000–2020 Land Cover and Land Use Change Dataset Derived from the Landsat Archive: First Results." *Frontiers in Remote Sensing* 3 (April). <https://doi.org/10.3389/frsen.2022.856903>.
- Prakash, M., S. Ramage, A. Kavvada, and S. Goodman. 2020. "Open Earth Observations for Sustainable Urban Development." *Remote Sensing* 12 (10): 1646. <https://doi.org/10.3390/rs12101646>.
- Runfola, D., A. Anderson, H. Baier, M. Crittenden, E. Dowker, S. Fuhrig, S. Goodman, et al. 2020. "GeoBoundaries: A Global Database of Political Administrative Boundaries." *PLOS ONE* 15 (4): e0231866. <https://doi.org/10.1371/journal.pone.0231866>.
- Salcedo-Sanz, S., P. Ghamisi, M. Piles, M. Werner, L. Cuadra, A. Moreno-Martínez, E. Izquierdo-Verdiguier, J. Muñoz-Marí, A. Mosavi, and G. Camps-Valls. 2020. "Machine Learning Information Fusion in Earth Observation: A Comprehensive Review of Methods, Applications and Data Sources." *Information Fusion* 63 (November): 256–72. <https://doi.org/10.1016/j.inffus.2020.07.004>.
- Sathyakumar, V., R. Ramsankaran, and R. Bardhan. 2020. "Geospatial Approach for Assessing Spatiotemporal Dynamics of Urban Green Space Distribution among Neighbourhoods: A Demonstration in Mumbai." *Urban Forestry & Urban Greening* 48 (February): 126585. <https://doi.org/10.1016/j.ufug.2020.126585>.
- Shindell, D.T. 2015. "The Social Cost of Atmospheric Release." *Climatic Change* 130 (2): 313–26. <https://doi.org/10.1007/s10584-015-1343-0>.

- Song, Y., and P. Wu. 2021. "Earth Observation for Sustainable Infrastructure: A Review." *Remote Sensing* 13 (8): 1528. <https://doi.org/10.3390/rs13081528>.
- Stanley, T., and D.B. Kirschbaum. 2017. "A Heuristic Approach to Global Landslide Susceptibility Mapping." *Natural Hazards* 87 (May): 145–64. <https://doi.org/10.1007/s11069-017-2757-y>.
- Sugiarto, W. 2022. "Impact of Wildlife Crossing Structures on Wildlife-Vehicle Collisions." *Transportation Research Record*, August. <https://doi.org/10.1177/03611981221108158>.
- Thomson, D.R., D.R. Leasure, T. Bird, N. Tzavidis, and A.J. Tatem. 2022. "How Accurate Are WorldPop-Global-Unconstrained Gridded Population Data at the Cell-Level? A Simulation Analysis in Urban Namibia." *PLOS ONE* 17 (7): e0271504. <https://doi.org/10.1371/journal.pone.0271504>.
- Thrasher, B., E.P. Maurer, C. McKellar, and P.B. Duffy. 2012. "Technical Note: Bias Correcting Climate Model Simulated Daily Temperature Extremes with Quantile Mapping." *Hydrology and Earth System Sciences* 16 (9): 3309–14. <https://doi.org/10.5194/hess-16-3309-2012>.
- Tsendbazar, N., L. Li, M. Koopman, S. Carter, M. Herold, I. Georgieva, and M. Lesiv. 2021. *WorldCover Product Validation Report, Version 1.1*. Paris: European Space Agency. [https://esa-worldcover.s3.eu-central-1.amazonaws.com/v100/2020/docs/WorldCover\\_PVR\\_V1.1.pdf](https://esa-worldcover.s3.eu-central-1.amazonaws.com/v100/2020/docs/WorldCover_PVR_V1.1.pdf).
- Tuholske, C., K. Caylor, C. Funk, A. Verdin, S. Sweeney, K. Grace, P. Peterson, and T. Evans. 2021. "Global Urban Population Exposure to Extreme Heat." *Proceedings of the National Academy of Sciences of the United States of America* 118 (41): e2024792118. <https://doi.org/10.1073/pnas.2024792118>.
- UNEP-WCMC (United Nations Environment Programme World Conservation Monitoring Centre) and IUCN (International Union for Conservation of Nature). n.d. (Database.) *Protected Planet: The World Database on Protected Areas (WDPA)*. <https://www.protectedplanet.net/>. Accessed October 4, 2022.
- UN-Habitat (United Nations Human Settlements Programme). 2020. *Metadata on SDGs Indicator 11.7.1*. Nairobi: UN-Habitat. [https://unhabitat.org/sites/default/files/2020/11/metadata\\_on\\_sdg\\_indicator\\_11.7.1\\_02-2020\\_1.pdf](https://unhabitat.org/sites/default/files/2020/11/metadata_on_sdg_indicator_11.7.1_02-2020_1.pdf).
- UN-Habitat. 2022. *Metadata on SDGs Indicator 15.1.1*. Nairobi: UN-Habitat. <https://unstats.un.org/sdgs/metadata/files/Metadata-15-01-01.pdf>.
- United Nations. n.d. "Goal 11." <https://sdgs.un.org/goals/goal11>. Accessed December 13, 2022.
- van der Kamp, J. 2017. *Social Cost-Benefit Analysis of Air Pollution Control Measures: Advancing Environmental-Economic Assessment Methods to Evaluate Industrial Point Emission Sources*. Karlsruhe, Germany: Karlsruher Institut für Technologie. <https://doi.org/10.5445/KSP/1000072046>.
- van Donkelaar, A., M.S. Hammer, L. Bindle, M. Brauer, J.R. Brook, M.J. Garay, N.C. Hsu, et al. 2021. "Monthly Global Estimates of Fine Particulate Matter and Their Uncertainty." *Environmental Science & Technology* 55 (22): 15287–300. <https://doi.org/10.1021/acs.est.1c05309>.
- Volin, E., A. Ellis, S. Hirabayashi, S. Maco, D.J. Nowak, J. Parent, and R.T. Fahey. 2020. "Assessing Macro-scale Patterns in Urban Tree Canopy and Inequality." *Urban Forestry & Urban Greening* 55 (November): 126818. <https://doi.org/10.1016/j.ufug.2020.126818>.
- Wang, C., Z.-H. Wang, and J. Yang. 2018. "Cooling Effect of Urban Trees on the Built Environment of Contiguous United States." *Earth's Future* 6 (8): 1066–81. <https://doi.org/10.1029/2018EF000891>.
- Wang, Y., C. Huang, Y. Feng, M. Zhao, and J. Gu. 2020. "Using Earth Observation for Monitoring SDG 11.3.1-Ratio of Land Consumption Rate to Population Growth Rate in Mainland China." *Remote Sensing* 12 (3): 357. <https://doi.org/10.3390/rs12030357>.
- Ward, P.J., H.C. Winsemius, S. Kuzma, M.F.P. Bierkens, A. Bouwman, H.D. Moel, A.D. Loaiza, et al. 2020. "Aqueduct Floods Methodology." Technical Note. Washington, DC: World Resources Institute. <https://www.wri.org/research/aqueduct-floods-methodology>.

---

Wellmann, T., A. Lausch, E. Andersson, S. Knapp, C. Cortinovis, J. Jache, S. Scheuer, et al. 2020. "Remote Sensing in Urban Planning: Contributions towards Ecologically Sound Policies?" *Landscape and Urban Planning* 204 (December): 103921. <https://doi.org/10.1016/j.landurbplan.2020.103921>.

WHO (World Health Organization). 2021. *WHO Global Air Quality Guidelines: Particulate Matter (PM<sub>2.5</sub> and PM<sub>10</sub>), Ozone, Nitrogen Dioxide, Sulfur Dioxide and Carbon Monoxide*. Geneva: WHO. <https://www.who.int/publications-detail-redirect/9789240034228>.

Wilson, S.J., E. Juno, J.-R. Pool, S. Ray, M. Phillips, S. Francisco, and S. McCallum. 2022. *Better Forests, Better Cities*. November. <https://www.wri.org/research/better-forests-better-cities>.

WorldPop. n.d. "WorldPop Global Population Data." Earth Engine Data Catalog. [https://developers.google.com/earth-engine/datasets/catalog/WorldPop\\_GP\\_100m\\_pop](https://developers.google.com/earth-engine/datasets/catalog/WorldPop_GP_100m_pop). Accessed November 8, 2022.

Zanaga, D., R. Van De Kerchove, W. De Keersmaecker, N. Souverijns, C. Brockmann, R. Quast, J. Wevers, et al. 2021. "ESA WorldCover 10 m 2020 V100." Zenodo. <https://doi.org/10.5281/zenodo.5571936>.

Zerger, A., and D.I. Smith. 2003. "Impediments to Using GIS for Real-Time Disaster Decision Support." *Computers, Environment and Urban Systems* 27 (2): 123–41. [https://doi.org/10.1016/S0198-9715\(01\)00021-7](https://doi.org/10.1016/S0198-9715(01)00021-7).

## ACKNOWLEDGMENTS

This research was made possible by the UrbanShift and Cities4Forests initiatives. We are thankful for the financial support to those initiatives from the Global Environment Facility and the UK Department for Environment, Food and Rural Affairs, respectively, which supported this research.

The authors would like to thank the reviewers and advisers who provided input on this research (unless otherwise noted, organizational affiliations are WRI): Becky Atkins, Ignacio Bernabe, Alejandra Bosch, Beatriz Cárdenas, Ingrid Coetzee (ICLEI), Gennadii Donchyts (Google), Jessica Ertel, Catyana Falsetti, Gloria Ferreyra, David Gibbs, Argyro Kavvada (NASA), Robin King, Samantha Kuzma, Jiaying Lin, Marc Manyifika, John-Rob Pool, Jaap Schellekens (Planet), Bongwiwe Simka (ICLEI), Gregory Taff, Wubanchi Tesso, and Mthobisi Wanda (ICLEI). Additionally, we would like to thank representatives of participant cities and liaisons who provided input on this research and presentations of the findings through surveys, focus groups, and interviews: Suryani Amin (ICLEI), Jessy Appavoo (C40 Cities), Ignacio Bernabe, Lara Caccia, Constant Cap (Code for Africa), Héctor Miguel Donado, Roger Mambeta Ndona, Bhaskar Padigala (ICLEI), Wubanchi Tesso, and Ji Xu (ICLEI).

Thanks also to the advisory group for the geospatial and data governance work of UrbanShift: Christoph Aubrecht (ESA), Zoltan Bartalis (ESA), Merlin Chatwin (Open North), Thomas Esch (German Aerospace Center), Dennis Mwaniki (UN-Habitat), Laura Parry (CDP), Steven Ramage (Group on Earth Observations), Stefaan Verhulst (New York University GovLab), and Dylan Weakley (City of Johannesburg).

Thanks also to the WRI program, technical, and operational staff who made this work and publication possible: Sadof Alexander, Timothy Anderegg, James Anderson, Logan Byers, Marc Daniels, Todd Gartner, Christopher Gillespie, Bruno Hernandez Incau, Manal Khan, Pablo Lazo, Beth Olberding, Mariana Orloff, John-Rob Pool, Emilia Suarez, and Deborah Valencia.

## ABOUT THE AUTHORS

**Eric Mackres** is Senior Manager for Data and Tools at WRI Ross Center for Sustainable Cities.

**Saif Shabou** is an Urban Data and Analytics Associate on the Data and Tools team at WRI Ross Center for Sustainable Cities.

**Ted Wong** is a Research and Project Associate on the Data and Tools team at WRI Ross Center for Sustainable Cities.

---

## ABOUT WRI

World Resources Institute is a global research organization that turns big ideas into action at the nexus of environment, economic opportunity, and human well-being.

### Our challenge

Natural resources are at the foundation of economic opportunity and human well-being. But today, we are depleting Earth's resources at rates that are not sustainable, endangering economies and people's lives. People depend on clean water, fertile land, healthy forests, and a stable climate. Livable cities and clean energy are essential for a sustainable planet. We must address these urgent, global challenges this decade.

### Our vision

We envision an equitable and prosperous planet driven by the wise management of natural resources. We aspire to create a world where the actions of government, business, and communities combine to eliminate poverty and sustain the natural environment for all people.

### Our approach

#### COUNT IT

We start with data. We conduct independent research and draw on the latest technology to develop new insights and recommendations. Our rigorous analysis identifies risks, unveils opportunities, and informs smart strategies. We focus our efforts on influential and emerging economies where the future of sustainability will be determined.

#### CHANGE IT

We use our research to influence government policies, business strategies, and civil society action. We test projects with communities, companies, and government agencies to build a strong evidence base. Then, we work with partners to deliver change on the ground that alleviates poverty and strengthens society. We hold ourselves accountable to ensure our outcomes will be bold and enduring.

#### SCALE IT

We don't think small. Once tested, we work with partners to adopt and expand our efforts regionally and globally. We engage with decision-makers to carry out our ideas and elevate our impact. We measure success through government and business actions that improve people's lives and sustain a healthy environment.



Copyright 2023 World Resources Institute. This work is licensed under the Creative Commons Attribution 4.0 International License. To view a copy of the license, visit <http://creativecommons.org/licenses/by/4.0/>